GEORGE C. MARSHALL SPACE FLIGHT CENTER

HUNTSVILLE, ALABAMA

September 30, 1960 M-NN-M-G&C-7-60

STUDY OF A SIMPLIFIED ATTITUDE CONTROL SYSTEM FOR A 24-HOUR SATELLITE

By

John Webster
and
David Schultz

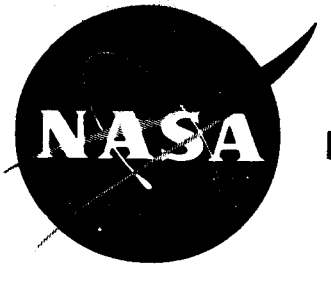

NATIONAL AERONAUTICS AND SPACE ADMINISTRATION

September 30, 1960 M-NN-M-G&C-7-60

STUDY OF A SIMPLIFIED ATTITUDE CONTROL SYSTEM FOR A 24-HOUR SATELLITE

By: John Webster and David N. Schultz
John Webster
Senior Engineer
David Schultz
Senior Engineer

Chrysler Corporation

Prepared By: W. E. Davis
W. E. Davis
Technical Writer

Illustrations By: Laura Smith
Laura Smith
Illustrator

OFFICE OF THE DIRECTOR
GUIDANCE AND CONTROL DIVISION

ABSTRACT

This document describes and defines a simplified attitude control system for a 24-hour satellite to be placed in an equatorial orbit about the earth. Efforts are made to establish operating characteristics for a generalized and theoretical satellite. Use of a theoretical satellite, without the restrictions of fixed configuration, permits the mathematical determination of the satellite's behavior and orbital tendencies.

The theoretical vehicle under study uses a three-axis flywheel-control system for attitude control. Roll and pitch reference is obtained from two earth horizon seekers. The sun is used for yaw reference. In addition to attitude control, orientation of solar cell banks for optimum sun energy transfer is included.

This document will endeavor to define and evaluate a theoretically workable system capable of maintaining both attitude control and solar-cell-bank orientation for a 24-hour orbit equatorial satellite.

TABLE OF CONTENTS

LIST OF ILLUSTRATIONS

TABLE OF SYMBOLS

Symbol	Definition	Units
X, Y, Z	Rotating reference axes	No units
ζ, η, γ	Space-fixed reference axes	No units
Ω	Earth's orbital rotational angle about the η-axis	Radians or Degrees
$\bar{X}, \bar{Y}, \bar{Z}$	Vehicle-fixed axes	No units
ϕ, θ, ψ	Vehicle rotational angles defined in Figure 2	Radians or Degrees
$\bar{X}', \bar{Y}', \bar{Z}'$	Intermediate reference axes defined in Figure 2	No units
a, b, c	Solar bank principal axes	No units
λ	Solar bank servo-drive angle defined in Figure 3	Radians or Degrees
E	Voltage output of a sensor element	Volts
ρ	Angle between sensor plane normal and incident sun ray	Radians
K	Sensor element constant	Volts
E_1	Voltage output of sensor face #1	Volts
E_2	Voltage output of sensor face #2	Volts
E_o	Difference between E_2 and E_1	Volts
$\bar{a}_1, \bar{b}_1, \bar{c}_1$	Yaw sensor face #1 coordinates defined in Figure 8	No Units
$\bar{a}_2, \bar{b}_2, \bar{c}_2$	Yaw sensor face #2 coordinates defined in Figure 8	No Units
μ	Inclination of yaw sensor faces, defined in Figure 8	Radians

Symbol	Definition	Units
A, B, C	Reference axes defined by Figure 10a	No units
$\bar{A}, \bar{B}, \bar{C}$	Reference axes defined by Figure 10b	No units
δ	Earth's orbital rotation angle about the sun, defined by Figure 10b	Radians or Degrees
d_{ij}	Elements of Matrix 1.5	No units
$\angle$	Indicates the angle measured between two axes	No units
$\Delta_r, \Delta_p, \Delta_y$	Sensed roll, pitch, and yaw angles	Radians
Ω'	Reference angle defined by Equation 1.26	Radians or Degrees
$(\Delta y)_{bias}$	Steady-state yaw bias term	Radians
$\bar{a}_1', \bar{b}_1', \bar{c}_1'$	Servo-drive sensor face #1 coordinates defined in Figure 11	No units
$\bar{a}_2', \bar{b}_2', \bar{c}_2'$	Servo-drive sensor face #2 coordinates defined in Figure 11	No units
μ'	Inclination of servo-drive sensor faces, defined in Figure 11	Radians
Δ_λ	Sensed servo-drive angle	Radians
$\cdot\cdot$	Dots over symbols indicate time derivatives	No units
$\vec{\omega}$	General instantaneous vehicle angular velocity	Rad/sec
$\omega_{\bar{X}}, \omega_{\bar{Y}}, \omega_{\bar{Z}}$	Components of $\vec{\omega}$ along vehicle axes $\bar{X}, \bar{Y}, \bar{Z}$	Rad/sec
$\omega_r, \omega_p, \omega_y$	Vehicle angular velocity about the roll, pitch and yaw axes	Rad/sec
m	The mass of a solar cell bank	Grams

Symbols	Definition	Units
d	The distance between the vehicle pitch axis ($\bar{Y}$) and solar bank a-axis	cm
l_1, l_2, l_3	Dimensions of solar cell bank, defined by Figure 13	cm
I_a, I_b, I_c	Principal moments of inertia of a solar cell bank along axes a, b, and c.	gm-cm sec^2
I_1, I_2, I_3	Total moments of inertia of the vehicle and both solar cell banks along $\bar{X}$, $\bar{Y}$, and $\bar{Z}$.	gm-cm sec^2
I_r, I_p, I_y	Vehicle moments of inertia about the roll, pitch and yaw axes.	gm-cm sec^2
I_F	Flywheel moment of inertia	gm-cm sec^2
$\alpha_r, \alpha_p, \alpha_y$	Roll, pitch and yaw flywheel angular displacements	Radians
J_r, J_p, J_y	Jet torques about the vehicle roll, pitch and yaw axes	gm-cm
D_r, D_p, D_y	Disturbance torques about the vehicle roll, pitch and yaw axes	gm-cm
$(\Delta_y)_{desired}$	Desired sensed yaw angle	Radians
Δ'_y	Compensated yaw signal	Radians
K_A	Yaw compensating amplifier gain	No units
$\dot{\lambda}_{max}$	Maximum limited solar bank angular velocity	Deg/min

INTRODUCTION

This report is the result of a study made on a simplified satellite control system. For any study of this type, certain basic assumptions must be made on which theoretical conclusions can be based.

Assume then, that a satellite is placed in a 24-hour equatorial orbit about the earth. The assumed satellite would use a three-axis-flywheel-type attitude control system obtaining its pitch and roll attitude stabilization by sensing the earth's horizon. Yaw attitude is obtained by referencing the sun.

Because of similarity to the previous "Three Axis Study of A Flywheel Type Attitude Control System", frequent references to this report will be made.

Since the most practical power source for such a satellite would be solar power, provisions are included to use the sun's rays and solar cells for this purpose. Two banks of solar cells are oriented toward the sun at all times, in order to obtain maximum energy transfer. Theoretical considerations indicate a relatively simple control system could be designed to sense and keep the solar cell banks oriented toward the sun.

With these factors in mind, mathematical analysis of the entire system can be undertaken.

DEFINITION OF ORBIT AND REFERENCE COORDINATES

The assumed satellite is launched into a 24-hour equatorial orbit. To locate the satellite's orbit with respect to the earth, a set of reference coordinates must be defined. The 24-hour equatorial satellite is a special type of orbit. The satellite lies in the earth's equatorial plane and it orbits the earth at the same rate as the earth rotates. It may therefore be seen that the satellite would remain seemingly fixed above a given subpoint at the equator.

The rotating reference axes X, Y, and Z, as illustrated in Figure 1, maintain constant rotation relative to the space-fixed reference frame ζ, η, and γ. At the vernal equinox, the ζ-axis is directed toward the sun and the ζ, γ-plane lies in the orbital plane. The orbital rotational angle Ω is about the η-axis, thus maintaining alignment of the η and Y axes. This relationship can then be expressed as:

1.1

$$\begin{bmatrix} X \\ Y \\ Z \end{bmatrix} = \begin{bmatrix} \cos\Omega & 0 & -\sin\Omega \\ 0 & 1 & 0 \\ \sin\Omega & 0 & \cos\Omega \end{bmatrix} \begin{bmatrix} \zeta \\ \eta \\ \gamma \end{bmatrix}$$

Consider $\bar{X}$, $\bar{Y}$, and $\bar{Z}$ to be vehicle fixed axes aligned with the vehicle's principal axes. Figure 2 illustrates the three rotational angles which are defined in the following sequence.

(YAW) 1. ϕ is a counterclockwise rotation about Z, re-orientating the body axes from X and Y to $\bar{X}'$ and $\bar{Y}'$, respectively.

(PITCH) 2. θ is a counterclockwise rotation about $\bar{Y}'$, re-orientating the body axes from Z and $\bar{X}'$, to $\bar{Z}'$ and $\bar{X}$, respectively.

(ROLL) 3. ψ is a counterclockwise rotation about $\bar{X}$ re-orientating the body axes from $\bar{Y}'$ and $\bar{Z}'$, to $\bar{Y}$ and $\bar{Z}$, respectively.

Thus the body-fixed axes may be specified as

1.2

$$\begin{bmatrix} \bar{X} \\ \bar{Y} \\ \bar{Z} \end{bmatrix} = \begin{bmatrix} \cos\phi\cos\theta & \sin\phi\cos\theta & -\sin\theta \\ \cos\phi\sin\theta\sin\psi - \sin\phi\cos\psi & \sin\phi\sin\theta\sin\psi + \cos\phi\cos\psi & \cos\theta\sin\psi \\ \cos\phi\sin\theta\cos\psi + \sin\phi\sin\psi & \sin\phi\sin\theta\cos\psi - \cos\phi\sin\psi & \cos\theta\cos\psi \end{bmatrix} \begin{bmatrix} X \\ Y \\ Z \end{bmatrix}$$

Substituting 1.1 into 1.2 gives

1.3

$$\begin{bmatrix} \bar{X} \\ \bar{Y} \\ \bar{Z} \end{bmatrix} = \begin{bmatrix} \cos\phi\cos\theta\cos\Omega - \sin\theta\sin\Omega & \sin\phi\cos\theta & -\cos\phi\cos\theta\sin\Omega - \sin\theta\cos\Omega \\ \cos\phi\sin\theta\sin\psi\cos\Omega - \sin\phi\cos\psi\cos\Omega + \cos\theta\sin\psi\sin\Omega & \sin\phi\sin\theta\sin\psi + \cos\phi\cos\psi & \sin\phi\cos\psi\sin\Omega - \cos\phi\sin\theta\sin\psi\sin\Omega + \cos\theta\sin\psi\cos\Omega \\ \cos\phi\sin\theta\cos\psi\cos\Omega + \sin\phi\sin\psi\cos\Omega + \cos\theta\cos\psi\sin\Omega & \sin\phi\sin\theta\cos\psi - \cos\phi\sin\psi & \cos\theta\cos\psi\cos\Omega - \sin\phi\sin\psi\sin\Omega - \cos\phi\sin\theta\cos\psi\sin\Omega \end{bmatrix} \begin{bmatrix} \zeta \\ \eta \\ \gamma \end{bmatrix}$$

This matrix orients the satellite's body-fixed control axes to the space-fixed axes and includes the orbital rotation angle Ω .

The orientation of the solar cell banks must now be examined. These solar cell banks are geometrically considered to be rectangular parallelepipeds. Consider axes a, b, and c aligned with the principal axes of the solar banks and b always aligned along the vehicle's $\bar{Y}$ axis which is the vehicle pitch axis. The servo-drive angle λ about $\bar{Y}$ will then specify the orientation of the solar banks relative to the vehicle. This is illustrated by Figure 3.

Thus

1.4

$$\begin{bmatrix} a \\ b \\ c \end{bmatrix} = \begin{bmatrix} \cos\lambda & 0 & \sin\lambda \\ 0 & 1 & 0 \\ -\sin\lambda & 0 & \cos\lambda \end{bmatrix} \begin{bmatrix} \bar{X} \\ \bar{Y} \\ \bar{Z} \end{bmatrix}$$

This expression defines the solar bank orientation with respect to the body-fixed axes.

Substitution of Matrix 1.4 into 1.3 gives the complete specification of the solar banks relative to the space fixed reference frame.

1.5

$$\begin{bmatrix} a \\ b \\ c \end{bmatrix} = \begin{bmatrix} (\cos\phi\cos\theta\cos\Omega - \sin\theta\sin\Omega)\cos\lambda + (\cos\phi\sin\theta\cos\psi\cos\Omega + \sin\phi\sin\psi\cos\Omega + \cos\theta\cos\psi\sin\Omega)\sin\lambda & \sin\phi\cos\theta\cos\lambda + (\sin\phi\sin\theta\cos\psi - \cos\phi\sin\psi)\sin\lambda & (\cos\theta\cos\psi\cos\Omega - \cos\phi\sin\theta\cos\psi\sin\Omega - \sin\phi\sin\psi\sin\Omega)\sin\lambda - (\cos\phi\cos\theta\sin\Omega + \sin\theta\cos\Omega)\cos\lambda \\ \cos\phi\sin\theta\sin\psi\cos\Omega - \sin\phi\cos\psi\cos\Omega + \cos\theta\sin\psi\sin\Omega & \sin\phi\sin\theta\sin\psi + \cos\phi\cos\psi & \sin\phi\cos\psi\sin\Omega + \cos\theta\sin\psi\cos\Omega - \cos\phi\sin\theta\sin\psi\sin\Omega \\ (\sin\theta\sin\Omega - \cos\phi\cos\theta\cos\Omega)\sin\lambda + (\cos\phi\sin\theta\cos\psi\cos\Omega + \sin\phi\sin\psi\cos\Omega + \cos\theta\cos\psi\sin\Omega)\cos\lambda & (\sin\phi\sin\theta\cos\psi - \cos\phi\sin\psi)\cos\lambda - \sin\phi\cos\theta\sin\lambda & (\cos\phi\cos\theta\sin\Omega + \sin\theta\cos\Omega)\sin\lambda + (\cos\theta\cos\psi\cos\Omega - \cos\phi\sin\theta\cos\psi\sin\Omega - \sin\phi\sin\psi\sin\Omega)\cos\lambda \end{bmatrix} \begin{bmatrix} \zeta \\ \eta \\ \gamma \end{bmatrix}$$

The differential servo drive and yaw sensors are mounted on the solar cell banks as illustrated in Figures 4 and 5. Therefore, this matrix is necessary to specify their outputs.

To express the output of the yaw sensor, consider Figures 6 and 7. Figure 6 illustrates the voltage output (E) of the sensor element as a function of the sun's incident angle (ρ). This relationship is expressed as

1.6

$$E = K \cos \rho$$

where K is a function of the sensing element used. The angle is measured from the normal of the sensor plane to the incident sun ray. Figure 7 illustrates the geometrical configuration of the yaw sensor and shows the resulting yaw signal output (E_o). The output is differential and may be expressed as

1.7

$$E_o = E_2 - E_1$$

where both E_1 and E_2 are given by Equation 1.6.

Since the yaw sensor is mounted on the solar cell bank, the fixed orientation of the two sensor faces relative to the solar cell bank coordinates may be determined. Figure 8 illustrates this relationship.

Consider axis $\bar{a}_1$ to be normal to the sensor #1 face and axis $\bar{a}_2$ to be normal to the sensor #2 face. Both sensor faces are inclined at an angle μ with respect to the solar cell bank b,c-plane. If both axes $\bar{c}_1$ and $\bar{c}_2$ are always aligned along axis c, then

1.8

$$\begin{bmatrix} \bar{a}_1 \\ \bar{b}_1 \\ \bar{c}_1 \end{bmatrix} = \begin{bmatrix} \cos\mu & -\sin\mu & 0 \\ \sin\mu & \cos\mu & 0 \\ 0 & 0 & 1 \end{bmatrix} \begin{bmatrix} a \\ b \\ c \end{bmatrix} \qquad \text{For Sensor \#1}$$

And

1.9

$$\begin{bmatrix}\bar{a}_2\\ \bar{b}_2\\ \bar{c}_2\end{bmatrix}=\begin{bmatrix}\cos\mu & \sin\mu & 0\\ -\sin\mu & \cos\mu & 0\\ 0 & 0 & 1\end{bmatrix}\begin{bmatrix}a\\ b\\ c\end{bmatrix} \qquad \text{For Sensor \#2}$$

If $\bar{A}$ is an axis parallel to the incident sun rays, then Equations 1.6 and 1.7 give the yaw sensor output as

1.10

$$E_o = K(\cos \angle \bar{a}_2, \bar{A} - \cos \angle \bar{a}_1, \bar{A})$$

where $\angle \bar{a}_1, \bar{A}$ is the angle between the $\bar{a}_1$-axis and $\bar{A}$-axis and $\angle \bar{a}_2, \bar{A}$ is the angle between the $\bar{a}_2$-axis and $\bar{A}$-axis.

Since Matrix 1.5 describes the relationship of the solar cell banks relative to space fixed coordinates, the direction of the incident sun rays ($\bar{A}$) with respect to the same space fixed coordinate set must now be determined. This would then completely specify the yaw sensor output as given by Equation 1.10.

Figure 9 provides a pictorial representation of the necessary coordinate systems. Consider δ as the orbital angle for describing the earth's motion about the sun. Because of the 23 1/2 degree inclination of the equatorial plane with respect to the ecliptic plane, two matrix transformations in terms of this angle and δ are necessary to locate $\bar{A}$ with respect to the ζ, η, γ-space-fixed coordinate system. This is demonstrated by Figure 10. The first transformation is given from Figure 10a as

1.11

$$\begin{bmatrix}A\\ B\\ C\end{bmatrix}=\begin{bmatrix}1 & 0 & 0\\ 0 & \cos 23\frac{1}{2}^\circ & \sin 23\frac{1}{2}^\circ\\ 0 & -\sin 23\frac{1}{2}^\circ & \cos 23\frac{1}{2}^\circ\end{bmatrix}\begin{bmatrix}\zeta\\ \eta\\ \gamma\end{bmatrix}$$

where ABC is a coordinate set such that A is aligned along ζ and B is normal to the plane of the ecliptic.

The second transformation is given from Figure 10b as

1.12

$$\begin{bmatrix}\bar{A}\\ \bar{B}\\ \bar{C}\end{bmatrix}=\begin{bmatrix}\cos\delta & 0 & -\sin\delta\\ 0 & 1 & 0\\ \sin\delta & 0 & \cos\delta\end{bmatrix}\begin{bmatrix}A\\ B\\ C\end{bmatrix}$$

where $\bar{A}\ \bar{B}\ \bar{C}$ is a coordinate set such that $\bar{B}$ is aligned along B and $\bar{A}$ is in the direction of the incident sun rays.

Combining Matrices 1.11 and 1.12 gives

1.13

$$\begin{bmatrix}\zeta\\ \eta\\ \gamma\end{bmatrix}=\begin{bmatrix}1 & 0 & 0\\ 0 & .917 & -.399\\ 0 & .399 & .917\end{bmatrix}\begin{bmatrix}\cos\delta & 0 & \sin\delta\\ 0 & 1 & 0\\ -\sin\delta & 0 & \cos\delta\end{bmatrix}\begin{bmatrix}\bar{A}\\ \bar{B}\\ \bar{C}\end{bmatrix}$$

or

$$\begin{bmatrix}\zeta\\ \eta\\ \gamma\end{bmatrix}=\begin{bmatrix}\cos\delta & 0 & \sin\delta\\ .399\sin\delta & .917 & -.399\cos\delta\\ -.917\sin\delta & .399 & .917\cos\delta\end{bmatrix}\begin{bmatrix}\bar{A}\\ \bar{B}\\ \bar{C}\end{bmatrix}$$

If Matrix 1.5 is re-written as

1.14

$$\begin{bmatrix}a\\ b\\ c\end{bmatrix}=\begin{bmatrix}d_{11} & d_{12} & d_{13}\\ d_{21} & d_{22} & d_{23}\\ d_{31} & d_{32} & d_{33}\end{bmatrix}\begin{bmatrix}\zeta\\ \eta\\ \gamma\end{bmatrix}$$

where the elements d_{ij} are given by the elements of Matrix 1.5,

then

1.15

$$\begin{bmatrix}\bar{a}_1\\ \bar{b}_1\\ \bar{c}_1\end{bmatrix}=\begin{bmatrix}\cos\mu & -\sin\mu & 0\\ \sin\mu & \cos\mu & 0\\ 0 & 0 & 1\end{bmatrix}\begin{bmatrix}d_{11} & d_{12} & d_{13}\\ d_{21} & d_{22} & d_{23}\\ d_{31} & d_{32} & d_{33}\end{bmatrix}\begin{bmatrix}\cos\delta & 0 & \sin\delta\\ .399\sin\delta & .917 & -.399\cos\delta\\ -.917\sin\delta & .399 & .917\cos\delta\end{bmatrix}\begin{bmatrix}\bar{A}\\ \bar{B}\\ \bar{C}\end{bmatrix}$$

And

1.16

$$\begin{bmatrix}\bar{a}_2\\ \bar{b}_2\\ \bar{c}_2\end{bmatrix}=\begin{bmatrix}\cos\mu & \sin\mu & 0\\ -\sin\mu & \cos\mu & 0\\ 0 & 0 & 1\end{bmatrix}\begin{bmatrix}d_{11} & d_{12} & d_{13}\\ d_{21} & d_{22} & d_{23}\\ d_{31} & d_{32} & d_{33}\end{bmatrix}\begin{bmatrix}\cos\delta & 0 & \sin\delta\\ .399\sin\delta & .917 & -.399\cos\delta\\ -.917\sin\delta & .399 & .917\cos\delta\end{bmatrix}\begin{bmatrix}\bar{A}\\ \bar{B}\\ \bar{C}\end{bmatrix}$$

Matrices 1.15 and 1.16 are derived by using Matrices 1.8, 1.9, 1.13 and 1.14 and are necessary to determine angles $\angle \bar{a}_1, \bar{A}$ and $\angle \bar{a}_2, \bar{A}$, respectively.

Multiplying out only the necessary terms of Matrices 1.15 and 1.16 gives

1.17

$$\begin{bmatrix}\\ \bar{a}_1\\ \\ \bar{b}_1\\ \bar{c}_1\end{bmatrix}=\begin{bmatrix}\cos\delta\left[d_{11}\cos\mu-d_{21}\sin\mu\right] & & \\ +.399\sin\delta\left[d_{12}\cos\mu-d_{22}\sin\mu\right] & — & — \\ -.917\sin\delta\left[d_{13}\cos\mu-d_{23}\sin\mu\right] & & \\ — & — & — \\ — & — & —\end{bmatrix}\begin{bmatrix}\\ \bar{A}\\ \\ \bar{B}\\ \bar{C}\end{bmatrix}$$

And

1.18

$$\begin{bmatrix} \\ \bar{a}_2 \\ \\ \bar{b}_2 \\ \bar{c}_2 \end{bmatrix} = \begin{bmatrix} \cos\delta\left[d_{11}\cos\mu + d_{21}\sin\mu\right] & & \\ +.399\sin\delta\left[d_{12}\cos\mu + d_{22}\sin\mu\right] & \text{---} & \text{---} \\ -.917\sin\delta\left[d_{13}\cos\mu + d_{23}\sin\mu\right] & & \\ & & \\ \text{---} & \text{---} & \text{---} \\ \text{---} & \text{---} & \text{---} \end{bmatrix} \begin{bmatrix} \\ \bar{A} \\ \\ \bar{B} \\ \bar{C} \end{bmatrix}$$

From Matrices 1.17 and 1.18

1.19

$$\cos\angle(\bar{a}_1, \bar{A}) = \cos\delta\left[d_{11}\cos\mu - d_{21}\sin\mu\right] + .399\sin\delta\left[d_{12}\cos\mu - d_{22}\sin\mu\right] - .917\sin\delta\left[d_{13}\cos\mu - d_{23}\sin\mu\right]$$

$$\cos\angle(\bar{a}_2, \bar{A}) = \cos\delta\left[d_{11}\cos\mu + d_{21}\sin\mu\right] + .399\sin\delta\left[d_{12}\cos\mu + d_{22}\sin\mu\right] - .917\sin\delta\left[d_{13}\cos\mu + d_{23}\sin\mu\right]$$

Therefore from Equation 1.10

1.20

$$E_0 = 2K\sin\mu\left[d_{21}\cos\delta + (.399d_{22} - .917d_{23})\sin\delta\right]$$

Substitution for the elements of d_{ij} from Matrix 1.5 gives

1.21

$$E_o = 2K\sin\mu\Big[\cos\delta(\cos\phi\sin\theta\sin\psi\cos\Omega - \sin\phi\cos\psi\cos\Omega + \cos\theta\sin\psi\sin\Omega)$$
$$+ \sin\delta(.917\cos\phi\sin\theta\sin\psi\sin\Omega - .917\sin\phi\cos\psi\sin\Omega - .917\cos\theta\sin\psi\cos\Omega$$
$$+ .399\cos\phi\cos\psi + .399\sin\phi\sin\theta\sin\psi)\Big]$$

This defines the desired voltage output (E_o) of the yaw sensor as a function of all variables.

If it is assumed that

1.22

$$E_o = 2K\sin\mu\sin\Delta_y \qquad \text{where } \Delta_y = \text{sensed yaw angle}$$

Then

1.23

$$\sin\Delta_y = \Big[(\cos\phi\sin\theta\sin\psi - \sin\phi\cos\psi)\cos\Omega + (\cos\theta\sin\psi)\sin\Omega\Big]\cos\delta$$
$$+ \Big[.917(\cos\phi\sin\theta\sin\psi - \sin\phi\cos\psi)\sin\Omega - .917(\cos\theta\sin\psi)\cos\Omega$$
$$+ .399(\cos\phi\cos\psi + \sin\phi\sin\theta\sin\psi)\Big]\sin\delta$$

For the special case of $\delta = 0^\circ$ (vernal equinox), Equation 1.23 reduces to

1.24

$$\sin\Delta_y = (\cos\phi\sin\theta\sin\psi - \sin\phi\cos\psi)\cos\Omega + (\cos\theta\sin\psi)\sin\Omega \qquad \text{for } \delta = 0^\circ$$

Reference to Matrix 1.5 shows that this sensed yaw angle may be defined as the complement of the angle between the incident sun rays (ζ-axis since $\delta = 0^o$) and the b-axis of the solar cell bank. This justifies the introduction of Equation 1.22.

The angle δ describes the changes of the yaw sensor output as the earth orbits the sun. Note that for $\delta = 90^o$ (summer solstice) the expression for the sensed yaw angle becomes

1.25

$$\sin\Delta_y = .917(\cos\phi\sin\theta\sin\psi - \sin\phi\cos\psi)\sin\Omega - .917(\cos\theta\sin\psi)\cos\Omega$$

$$+.399(\cos\phi\cos\psi + \sin\phi\sin\theta\sin\psi) \qquad \text{for } \delta = 90^\circ$$

Comparison of Equation 1.25 with Equation 1.24 shows that there is an effective phase shift of 90^o for the reference point of Ω and that there is an added bias term of $.399(\cos\phi\cos\psi + \sin\phi\sin\theta\sin\psi)$. For ϕ, θ and ψ small, this bias term becomes the constant value of .399 when $\delta = 90^o$. By then defining a new reference angle Ω' such that

1.26

$$\Omega = 90^\circ + \Omega' \qquad \text{for } \delta = 90^\circ$$

Equation 1.25 may be re-written as

1.27

$$\sin\Delta_y = .917(\cos\phi\sin\theta\sin\psi - \sin\phi\cos\psi)\cos\Omega' + .917(\cos\theta\sin\psi)\sin\Omega'$$

$$+.399(\cos\phi\cos\psi + \sin\phi\sin\theta\sin\psi) \qquad \text{for } \delta = 90^\circ$$

If Equations 1.27 and 1.24 are now compared, they are found to be quite similar, especially if the bias term is removed by biasing the yaw sensor an equal but opposite amount. This biasing may be accomplished either by using an internal time reference or by control from a ground station. The only differences then are the .917 attenuation term and the effective phase shift of the $\Omega = 0^o$ reference point. As far as the vehicle's attitude relative to the earth is concerned, this reference phase shift

is ignorable. Therefore, by using bias and increasing the gain as a function of δ, equation 1.24 may be interpreted as valid for all δ such that $0 \leq \delta \leq 90^{o}$. With similar reasoning and including the bias and gain increase considerations, Equation 1.24 may be extended to apply for all values of δ. Thus,

1.28

$$\sin\Delta_y = (\cos\phi\sin\theta\sin\psi - \sin\phi\cos\psi)\cos\Omega + (\cos\theta\sin\psi)\sin\Omega \qquad \text{for all } \delta$$

where as a function of δ the necessary steady-state bias term is given by $(\Delta_y)_{bias} = .399\sin\delta$ and can be subtracted from the sensed yaw angle.

As in the previous progress report, the sensed pitch angle is the complement of the angle between the Z-axis and the $\bar{X}$-axis. The sensed roll angle is the complement of the angle between the Z-axis and the $\bar{Y}$-axis. Using a direction cosine matrix comparison with Equations 1.2, these sensed angles may be written as

1.29

$$\Delta_p = -\theta \qquad \text{where } \Delta_p = \text{sensed pitch angle}$$

$$\sin\Delta_r = \cos\theta\sin\psi \qquad \text{where } \Delta_r = \text{sensed roll angle}$$

Therefore the complete expressions for the sensed attitude angles become

1.30

$$\sin\Delta_y = (\cos\phi\sin\theta\sin\psi - \sin\phi\cos\psi)\cos\Omega + \sin\Delta_r\sin\Omega$$

$$\Delta_p = -\theta$$

$$\sin\Delta_r = \cos\theta\sin\psi$$

Even though the use of bias and gain increase for the yaw sensor removed unwanted terms in the control loop, there will still be a power loss from the solar cell bank as a function of δ. This is because the incident sun rays do not remain

perpendicular to the solar banks as the earth orbits the sun. Since the maximum voltage loss is less than 9%, there will be a maximum power loss of approximately 16% occurring at the $\delta = 90^{\circ}$ and $\delta = 270^{\circ}$ points (summer and winter solstice, respectively). When $\delta = 0^{\circ}$ or $\delta = 180^{\circ}$ (vernal and autumnal equinox) the sunlight is again perpendicular to the solar banks and full power output of the solar cells can be achieved.

Observing Equation 1.30, note that the sensed yaw angle (Δ_y) is independent of the servo-drive-loop signal (λ). Also, both pitch and roll sensed angles (Δ_p and Δ_r) are independent of the angle ϕ which is always about the Z-axis (local vertical axis). Pitch and roll angles are also independent of the orbital angle of revolution (Ω). This is a direct consequence of the defined sensor angles.

The expression for sensed vehicle yaw (Δ_y) presents some interesting cases. First consider $\Omega = 0^{\circ}$ as illustrated by Figures 1 and 4. Then from Equations 1.30

1.31

$$\sin\Delta_y = \cos\phi\sin\theta\sin\psi - \sin\phi\cos\psi \qquad \text{for } \Omega = 0^{\circ}$$

which for small angles (i.e. all angles $\rightarrow 0$) reduces to

1.32

$$\Delta_y = \theta\psi - \phi \qquad \text{for } \Omega = 0^{\circ}$$

This shows that the sensed yaw signal is primarily $-\phi$, since for small angles $\phi >> \theta\psi$. When the pitch and roll channels are nulled, this becomes exact and

1.33

$$\Delta_y = -\phi \qquad \text{for } \Omega = 0^{\circ}, \ \theta = \psi = 0$$

Next consider the case for $\Omega = 90^\circ$. This condition is illustrated by Figures 1 and 5. Then from Equations 1.30

1.34

$$\sin\Delta_y = \sin\Delta_r \qquad \text{for } \Omega = 90^\circ$$

$$\therefore \Delta_y = \Delta_r$$

For this condition all sensed vehicle roll is coupled into the yaw control loop causing yaw rotation about the Z-axis. This represents a state of confusion since the yaw sensor is unable to see the vehicle yaw rotation and as a result there is no yaw control for $\Omega = 90^\circ$.

When $\Omega = 180^\circ$, Equation 1.30 shows that

1.35

$$\sin\Delta_y = -\cos\phi\sin\theta\sin\psi + \sin\phi\cos\psi \qquad \text{for } \Omega = 180^\circ$$

Note that the polarity sense of Δ_y in Equation 1.35 is the negative of that in Equation 1.31. This polarity inversion occurs as soon as Ω exceeds 90° because of the $\cos\Omega$ term in Equation 1.30. Consequently ϕ is controlled to 180°, $\bar{X}$ is controlled to $-X$, $\bar{Y}$ is controlled to $-Y$, and $\bar{Z}$ is controlled to $+Z$ for this yaw polarity inversion. This shows, then, that the vehicle must rotate 180° about the Z-axis after Ω exceeds 90°.

When $\Omega = 270^\circ$, the yaw expression in equation 1.30 reduces to

1.36

$$\sin\Delta_y = -\cos\theta\sin\psi = -\sin\Delta_r \qquad \text{for } \Omega = 270^\circ$$

$$\therefore \Delta_y = -\Delta_r$$

For this condition of $\Omega = 270^{\circ}$, any sensed vehicle roll is negatively coupled into the yaw control loop causing yaw rotation about the Z-axis. This also represents a state of confusion caused by the absence of yaw control at $\Omega = 270^{\circ}$. For the same rotation caused by the roll disturbance, Equation 1.36 is of opposite sign to Equation 1.34. Thus, after the vehicle passes the $\Omega = 270^{\circ}$ point, there must be another 180° rotation about the Z-axis. Therefore, ϕ will again be controlled to 0° and $\overline{X}$, $\overline{Y}$,$\overline{Z}$, controlled to XYZ until the $\Omega = 90^{\circ}$ point is again reached.

The development for the servo-drive-sensor output is similar to that for yaw sensor output. The sensing element and geometrical configuration are again given by Figures 6 and 7, respectively. The relationship of the sensor relative to the solar cell bank is given by Figure 11. Let $\overline{a}_1'$ and $\overline{a}_2'$ be perpendicular to sensor #1 face and sensor #2 face, respectively. Both sensor faces are inclined at an angle μ' with respect to the solar-cell-bank b,c-plane. If both axes $\overline{b}_1'$ and $\overline{b}_2'$ are always aligned along axis b, then

1.37

$$\begin{bmatrix} \overline{a}_1' \\ \overline{b}_1' \\ \overline{c}_1' \end{bmatrix} = \begin{bmatrix} \cos\mu' & 0 & -\sin\mu' \\ 0 & 1 & 0 \\ \sin\mu' & 0 & \cos\mu' \end{bmatrix} \begin{bmatrix} a \\ b \\ c \end{bmatrix} \qquad \text{FOR SENSOR \#1}$$

And

1.38

$$\begin{bmatrix} \overline{a}_2' \\ b_2' \\ c_2' \end{bmatrix} = \begin{bmatrix} \cos\mu' & 0 & \sin\mu' \\ 0 & 1 & 0 \\ -\sin\mu' & 0 & \cos\mu' \end{bmatrix} \begin{bmatrix} a \\ b \\ c \end{bmatrix} \qquad \text{FOR SENSOR \#2}$$

Now Equation 1.10 is also valid for the servo-drive-sensor output. In order to determine the necessary angles, the following matrices are written

1.39

$$\begin{bmatrix} \bar{a}_1' \\ \bar{b}_1' \\ \bar{c}_1' \end{bmatrix} = \begin{bmatrix} \cos\mu' & 0 & -\sin\mu' \\ 0 & 1 & 0 \\ \sin\mu' & 0 & \cos\mu' \end{bmatrix} \begin{bmatrix} d_{11} & d_{12} & d_{13} \\ d_{21} & d_{22} & d_{23} \\ d_{31} & d_{32} & d_{33} \end{bmatrix} \begin{bmatrix} \cos\delta & 0 & \sin\delta \\ .399\sin\delta & .917 & -.399\cos\delta \\ -.917\sin\delta & .399 & .917\cos\delta \end{bmatrix} \begin{bmatrix} \bar{A} \\ \bar{B} \\ \bar{C} \end{bmatrix}$$

And

1.40

$$\begin{bmatrix} \bar{a}_2' \\ \bar{b}_2' \\ \bar{c}_2' \end{bmatrix} = \begin{bmatrix} \cos\mu' & 0 & \sin\mu' \\ 0 & 1 & 0 \\ -\sin\mu' & 0 & \cos\mu' \end{bmatrix} \begin{bmatrix} d_{11} & d_{12} & d_{13} \\ d_{21} & d_{22} & d_{23} \\ d_{31} & d_{32} & d_{33} \end{bmatrix} \begin{bmatrix} \cos\delta & 0 & \sin\delta \\ .399\sin\delta & .917 & -.399\cos\delta \\ -.917\sin\delta & .399 & .917\cos\delta \end{bmatrix} \begin{bmatrix} \bar{A} \\ \bar{B} \\ \bar{C} \end{bmatrix}$$

where again the d_{ij} elements are given by Equation 1.5, δ is the earth's orbital angle about the sun, and $\bar{A}$ is the direction of the incident sun rays on the sensor elements.

Multiplying out only the necessary terms of Equation 1.39 gives

1.41

$$\begin{bmatrix} \\ \bar{a}_1' \\ \\ \bar{b}_1' \\ \bar{c}_1' \end{bmatrix} = \begin{bmatrix} \cos\delta\left[d_{11}\cos\mu' - d_{31}\sin\mu'\right] & & \\ +\sin\delta\left[.399(d_{12}\cos\mu' - d_{32}\sin\mu') - .917(d_{13}\cos\mu' - d_{33}\sin\mu')\right] & --- & --- \\ --- & --- & --- \\ --- & --- & --- \end{bmatrix} \begin{bmatrix} \bar{A} \\ \bar{B} \\ \bar{C} \end{bmatrix}$$

Replacing μ' with $-\mu'$ in Equation 1.41 also solves Matrix 1.40 giving

1.42

$$\begin{bmatrix} \bar{a}_2' \\ \bar{b}_2' \\ \bar{c}_2' \end{bmatrix} = \begin{bmatrix} \cos\delta\left[d_{11}\cos\mu' + d_{31}\sin\mu'\right] & & \\ +\sin\delta\left[.399(d_{12}\cos\mu' + d_{32}\sin\mu') - .917(d_{13}\cos\mu' + d_{33}\sin\mu')\right] & --- & --- \\ --- & --- & --- \\ --- & --- & --- \end{bmatrix} \begin{bmatrix} \bar{A} \\ \bar{B} \\ \bar{C} \end{bmatrix}$$

Thus Matrices 1.41 and 1.42 give the angles $\angle \bar{a}_1', \bar{A}$ and $\angle \bar{a}_2', \bar{A}$, respectively.

Substitution of these angles into Equation 1.10 with the replacement of $\bar{a}_2'$ for $\bar{a}_2$ and $\bar{a}_1'$ for $\bar{a}_1$ gives

1.43

$$\begin{aligned} E_0 &= K\left[\cos\angle \bar{a}_2', \bar{A} - \cos\angle \bar{a}_1', \bar{A}\right] \\ &= K\Big[\cos\delta(d_{11}\cos\mu' + d_{31}\sin\mu') + \sin\delta\left\{.399(d_{12}\cos\mu' + d_{32}\sin\mu') - .917(d_{13}\cos\mu' + d_{33}\sin\mu')\right\} \\ &\quad - \cos\delta(d_{11}\cos\mu' - d_{31}\sin\mu') - \sin\delta\left\{.399(d_{12}\cos\mu' - d_{32}\sin\mu') - .917(d_{13}\cos\mu' - d_{33}\sin\mu')\right\}\Big] \end{aligned}$$

Collecting terms in Equation 1.43 gives

1.44

$$E_0 = 2K\sin\mu'\left[d_{31}\cos\delta + .399d_{32}\sin\delta - .917d_{33}\sin\delta\right]$$

Finally, substituting the values d_{ij} from Matrix 1.5 gives

1.45

$$E_o = 2K\sin\mu'\Big[\cos\delta\Big\{(\sin\theta\sin\Omega-\cos\phi\cos\theta\cos\Omega)\sin\lambda+(\cos\phi\sin\theta\cos\psi\cos\Omega +\sin\phi\sin\psi\cos\Omega+\cos\theta\cos\psi\sin\Omega)\cos\lambda\Big\} +\sin\delta\Big\{.399(-\sin\phi\cos\theta\sin\lambda+\sin\phi\sin\theta\cos\psi\cos\lambda-\cos\phi\sin\psi\cos\lambda) -.917(\cos\phi\cos\theta\sin\Omega+\sin\theta\cos\Omega)\sin\lambda-.917(\cos\theta\cos\psi\cos\Omega -\cos\phi\sin\theta\cos\psi\sin\Omega-\sin\phi\sin\psi\sin\Omega)\cos\lambda\Big\}\Big]$$

If it is again assumed that

1.46

$$E_o = 2K\sin\mu'\sin\Delta_\lambda \qquad \text{where } \Delta_\lambda = \text{the sensed servo drive angle}$$

Then for $\delta = 0^o$.

1.47

$$\sin\Delta_\lambda = \cos\phi\sin\theta\cos\psi\cos\Omega\cos\lambda+\sin\phi\sin\psi\cos\Omega\cos\lambda +\cos\theta\cos\psi\sin\Omega\cos\lambda+\sin\theta\sin\Omega\sin\lambda-\cos\phi\cos\theta\cos\Omega\sin\lambda$$

Or

$$\sin\Delta_\lambda = \cos\Omega\Big[\cos\phi\sin\theta\cos\psi\cos\lambda+\sin\phi\sin\psi\cos\lambda-\cos\phi\cos\theta\sin\lambda\Big] +\sin\Omega\Big[\cos\theta\cos\psi\cos\lambda+\sin\theta\sin\lambda\Big]$$

With similar reasoning as that for the sensed yaw angle (Δ_y), Equation 1.47 can be extended to be valid for all δ. The use of bias is, however, not necessary since all terms in Equation 1.45 multiplied by the factor .399 vanish as ϕ, θ , and ψ are nulled.

As the vehicle orbits the earth, it has previously been shown that there are two values for the ϕ null position.

For $-90^\circ < \Omega < +90^\circ$, ϕ is controlled to 0°

For $+90^\circ < \Omega < 270^\circ$, ϕ is controlled to 180°.

In addition, if both θ and ψ are set equal to zero, Equation 1.47 separates into two cases,

1.48

CASE I $\quad \sin\Delta_\lambda = \sin\Omega\cos\lambda - \cos\Omega\sin\lambda$

$\sin\Delta_\lambda = \sin(\Omega-\lambda)$ $\quad$ for $-90^\circ<\Omega<+90^\circ$

$\therefore \Delta_\lambda = \Omega-\lambda$ $\quad$ and $\phi=\theta=\psi=0^\circ$

CASE II $\quad \sin\Delta_\lambda = \sin\Omega\cos\lambda + \cos\Omega\sin\lambda$

$\sin\Delta_\lambda = \sin(180^\circ - \Delta_\lambda) = \sin(\Omega+\lambda)$ $\quad$ for $+90^\circ<\Omega<+270^\circ$

$\therefore \Delta_\lambda = 180^\circ-(\Omega+\lambda)$ $\quad$ and $\phi = 180^\circ$

$\theta=\psi=0^\circ$

In order to null the sensed servo drive signal, these equations show that the control loop must enforce

1.49

CASE I $\quad \lambda=\Omega \quad \therefore \dot\lambda = \dot\Omega$ $\quad$ for $-90^\circ<\Omega<+90^\circ$

and $\phi=\theta=\psi=0^\circ$

CASE II $\quad \lambda = 180^\circ-\Omega \quad \therefore \dot\lambda = -\dot\Omega$ $\quad$ for $90^\circ<\Omega<270^\circ$

and $\phi = 180^\circ$

$\theta=\psi=0^\circ$

It is then evident that the solar cell banks are driven at the same rate as the orbital angular velocity for $-90^\circ < \Omega < +90^\circ$. However, when $90^\circ < \Omega < 270^\circ$, the velocity of the solar cell banks changes sign. In this interval, the solar cell banks are driven at a rate equal and opposite to the orbital angular velocity. This velocity reversal is automatic since there is a 180° phase shift

of the sensed servo-drive signal each time the vehicle rotates about a confusion point. For steady-state nulled conditions, the relationship of the solar bank coordinates (a,b,c) to the vehicle axes ($\bar{X},\bar{Y},\bar{Z}$) as the vehicle orbits the earth is illustrated by Figure 12.

Since $\sin\lambda = \sin\Omega$ for steady-state operation, λ may be used to resolve the yaw and roll signals as the vehicle orbits the earth. This is developed in the conclusion of this report and gives the sensed yaw signal priority over the sensed roll signal on both sides of the "confused" yaw sensor positions ($\Omega = 90^{\circ}$ and $\Omega = 270^{\circ}$).

As shown by the previous progress report, the components of the general instantaneous-vehicle-angular velocity $\vec{\omega}$ referenced to the moving vehicle axes $\bar{X}$, $\bar{Y}$, and $\bar{Z}$ are

1.50

$$\omega_r = \omega_{\bar{x}} = \dot{\psi} - \dot{\phi}\sin\theta$$

$$\omega_p = \omega_{\bar{y}} = \dot{\phi}\cos\theta\sin\psi + \dot{\theta}\cos\psi$$

$$\omega_y = \omega_{\bar{z}} = \dot{\phi}\cos\theta\cos\psi - \dot{\theta}\sin\psi$$

Also developed in the same report were the angular velocity equations, including the orbital velocity $\dot{\Omega}$ as

1.51

$$\omega_r = \dot{\psi} - \dot{\phi}\sin\theta + \dot{\Omega}\sin\phi\cos\theta$$

$$\omega_p = \dot{\theta}\cos\psi + \dot{\phi}\cos\theta\sin\psi + \dot{\Omega}(\sin\phi\sin\theta\sin\psi + \cos\phi\cos\psi)$$

$$\omega_y = \dot{\phi}\cos\theta\cos\psi - \dot{\theta}\sin\psi + \dot{\Omega}(\sin\phi\sin\theta\cos\psi - \cos\phi\sin\psi)$$

where ω_r, ω_p, and ω_y are the rotational velocity components about the body-fixed control axes.

The sensor outputs and the angular velocity components have been expressed in terms of the three independent-rotational angles ϕ, θ, and ψ and the orbital position angle Ω. These will be used later to develop the complete torque equations.

As mentioned previously, each solar cell bank is considered to be a homogeneous rectangular parallelepiped as shown in Figure 13. With reference to Figure 13, let m be the mass of each solar cell bank. As introduced previously, a,b,c is an orthogonal coordinate set fixed in the solar cell bank and aligned to the bank's principal axes with b aligned along the vehicle fixed $\bar{Y}$-axis. Let d be the distance between the $\bar{X}$ and a axes. Consider l_1, l_2, and l_3 to be the dimensions of the solar bank as illustrated. Define I_a, I_b, and I_c to be the principal moments of inertia of the solar cell bank along a, b, and c, respectively.

Thus, the moments of inertia can be written as

1.52

$$I_a = \frac{m(l_2^2+l_3^2)}{12}$$

$$I_b = \frac{m(l_1^2+l_3^2)}{12}$$

$$I_c = \frac{m(l_1^2+l_2^2)}{12}$$

Defining I_1, I_2 and I_3 to be the total moments of inertia of the vehicle and both solar cell banks referenced to the vehicle axes $\bar{X}$, $\bar{Y}$, and $\bar{Z}$, respectively, and considering the a-axis aligned in the $\bar{X}$-direction gives:

1.53

$$I_1 = I_r + 2(I_a + md^2)$$

$$I_2 = I_p + 2(I_b) \qquad \text{for } \lambda = 0°$$

$$I_3 = I_y + 2(I_c + md^2)$$

where I_r, I_p, I_y are the moments of inertia of only the vehicle about the roll, pitch and yaw axes, respectively.

After the solar-cell bank has rotated 90° (i.e. $\lambda = 90^\circ$) the a-axis is then aligned to the $\bar{Z}$-axis direction, and the equation becomes

1.54

$$I_1 = I_r + 2(I_c + md^2)$$

$$I_2 = I_p + 2(I_b) \qquad \text{for } \lambda = 90^\circ$$

$$I_3 = I_y + 2(I_a + md^2)$$

Equations 1.53 and 1.54 portray the maximum variation of inertia about the vehicle's principal axes caused by the solar-cell-bank rotation. Note that I_2 (the moment of inertia along the $\bar{Y}$-axis) remains constant, but there is a continuous interchange between I_1 and I_3 as the bank rotates. This interchange is caused by the difference between I_a and I_c as described by Equations 1.52.

These equations also indicate a preferable configuration for the solar bank in order to minimize this inertia change. This would be accomplished by making I_2 large with respect to both I_1 and I_3, thus making the difference between I_a and I_b small.

Since the angle λ can be instrumented, this variation in inertia could be continuously compensated by gain changes. Whether or not this is necessary depends upon the magnitude of these inertia variations.

The torque expressions derived in the previous progress report merely need modification of the moment of inertia quantities in order to contain inertia variations shown by Equations 1.53 and 1.54. These changes are shown by

1.55

$$\dot{\omega}_r I_1 = -I_F \ddot{\alpha}_r - \omega_p \omega_y (I_3 - I_2) + \dot{\alpha}_p \omega_y I_F - \dot{\alpha}_y \omega_p I_F + J_r + D_r$$

$$\dot{\omega}_p I_2 = -I_F \ddot{\alpha}_p + \omega_y \omega_r (I_3 - I_1) - \dot{\alpha}_r \omega_y I_F + \dot{\alpha}_y \omega_r I_F + J_p + D_p$$

$$\dot{\omega}_y I_3 = -I_F \ddot{\alpha}_y - \omega_r \omega_p (I_2 - I_1) + \dot{\alpha}_r \omega_p I_F - \dot{\alpha}_p \omega_r I_F + J_y + D_y$$

where I_1, I_2, and I_3 are varied parameters, with maximum deviations given by Equations 1.53 and 1.54. I_F is the flywheel moment of inertia; $\dot{\alpha}$ is the indicated flywheel speed and $\ddot{\alpha}$ is the indicated flywheel acceleration. The indicated J and D terms are jet and disturbance torques.

The servo-drive loop is considered to be slow relative to the vehicle attitude-control system. Therefore, the vehicle roll and yaw cross-coupling disturbances (because of the solar bank's rotation) may be neglected. Thus the servo-drive torque disturbs the vehicle only about the pitch axis. Since friction is an internal loss, only the acceleration of the solar-cell bank by the servo-drive system will provide vehicle pitch disturbance. Adding this acceleration term to Equation 1.55 gives

1.56

$$\dot{\omega}_r I_1 = -I_F \ddot{\alpha}_r - \omega_p \omega_y (I_3 - I_2) + \dot{\alpha}_p \omega_y I_F - \dot{\alpha}_y \omega_p I_F + J_r + D_r$$

$$\dot{\omega}_p I_2 = -I_F \ddot{\alpha}_p + \omega_y \omega_r (I_3 - I_1) - \dot{\alpha}_r \omega_y I_F + \dot{\alpha}_y \omega_r I_F + 2 I_b \ddot{\lambda} + J_p + D_p$$

$$\dot{\omega}_y I_3 = -I_F \ddot{\alpha}_y - \omega_r \omega_p (I_2 - I_1) + \dot{\alpha}_r \omega_p I_F - \dot{\alpha}_p \omega_r I_F + J_y + D_y$$

This equation formulates the complete torque expression.

CONCLUSION

Previous mathematical equations and explanations have defined a theoretically workable control system for a 24-hour satellite in an equatorial orbit. Since the sun is used for yaw-reference, there are two confusion points($\Omega = 90^\circ$ and $\Omega = 270^\circ$) at which yaw control is lost. There is also a yaw reference polarity reversal at these two points so that the vehicle must rotate 180° about its yaw axis each time a confusion point is passed. Because of these vehicle rotations, the solar banks never rotate more than 180° as they are continuously driven to face the incident sunlight. Therefore, in order to transfer the solar-cell generated power into the vehicle, direct interconnecting wires or cables may be used. This can be an advantage, since if the solar banks had to continuously rotate, some type of slip ring arrangement would have to be used, resulting in moving parts subject to wear.

The major disadvantages resulting from yaw-referencing the sun are the yaw-sensitivity decline and roll-coupling increase into the yaw sensor as the confusion points are approached. Reference to Figure 14 will reveal both the yaw-sensitivity decline and the roll-coupling increase into the yaw loop as the $\Omega = 90^\circ$ confusion point is approached. In order to improve yaw-control sensitivity for normal steady-state operation, an investigation of compensating networks was made. This investigation produced a roll-coupling rejection and sensor-gain-compensation network which is illustrated by Figure 15. The resolving network is

based on a function of solar-bank-axle angle λ which is an available input and for steady-state operation is equivalent to the satellite's orbital angle Ω. Assuming steady-state conditions and small angle disturbances, Equation 1.28 may be reduced to

1.57

$$\Delta_y = (\Delta_y)_{desired} \cos\Omega + \Delta_r \sin\Omega \qquad \text{where} \quad \sin\Delta_y \approx \Delta_y \quad \text{and} \quad \sin\Delta_r \approx \Delta_r$$

If the sensed roll signal Δ_r is now multiplied by $\sin\lambda$ and subtracted from Equation 1.57, the roll coupling into the yaw control loop is effectively rejected assuming either $\lambda = \Omega$ or $\lambda = (180^\circ - \Omega)$. However, the desired yaw signal $(\Delta_y)_{desired}$ still falls off as a cosine function of Ω. Thus, to keep the yaw sensor gain relatively constant as the $\Omega = 90^\circ$ confusion point is approached, an implicit resolving loop may be used to provide yaw gain compensation. This compensating loop is also illustrated in Figure 15 where the final yaw output signal may be expressed as

1.58

$$\Delta'_y = \frac{K_A (\Delta_y)_{desired} \cos\Omega}{1 + K_A \cos\lambda}$$

The constant value K_A represents the amplifier gain. As this gain becomes very large, $\Delta'_y \rightarrow (\Delta_y)_{desired}$ for all Ω assuming steady state conditions. Equation 1.58 is also plotted in Figure 14 as a relative yaw signal gain for the value of K_A arbitrarily equal to 20. This shows that the compensated yaw gain is relatively flat as the satellite approaches the $\Omega = 90^\circ$ point and the gain is still in excess of 60% at $\pm 5^\circ$ on either side of this confusion point.

Figure 16 is also included to illustrate the amount of gain compensation for $K_A = 20$. Of course, no amount of compensation can result in sensed yaw signal at the confusion point, since the amplifier gain cannot become infinite. This represents an appreciable improvement in yaw sensitivity, however, since the area of yaw control loss in the control system is reduced to a space of only approximately 10° at each confusion point. An optimim value for K_A would of course depend upon the satellite's mission specifications concerning yaw gain as a function of Ω.

The primary requirement for "tight" yaw control is to properly orient the jet thrust vector when the satellite's orbital velocity must be changed. This velocity change might become necessary for either a desirable orbital maneuver or an orbital velocity correction caused by jet thrust errors.

Assume the satellite to be in the 24-hour equatorial orbit and it becomes desirable to shift its position from one point to another over the earth's equator. This shift in position is started by either increasing or decreasing the orbital velocity of the satellite through the use of some type of jets. The satellite's orbit is now elliptical. After a specified number of revolutions and, when the satellite is over the desired point on earth, an equal and opposite jet thrust must be applied in order to circularize the orbit again. If the satellite is to remain in the equatorial plane, the jets must be properly oriented. Therefore, any changes in orbital velocity should be made only while tight yaw control of the vehicle is maintained. Use of roll-coupling rejection and yaw gain compensation as explained earlier reduces the areas of yaw confusion to about $\pm$ 5 degrees on each side of the confusion points ($\Omega = 90^{\circ}$ and $\Omega = 270^{\circ}$). This gives approximately two-10 degree areas of confusion lasting for 40 minutes each. Of course these areas may be reduced by increasing K_A.

Any changes in orbital velocity of the satellite at any point other than the two confusion areas would present no control system problems, since both the yaw gain and sensitivity are high. It must be presumed, though, that it could become necessary to initiate orbital changes or velocity corrections while the satellite was within a confusion area. In this area, yaw control is not only poor, but the vehicle must rotate 180° about the yaw axis because of the yaw-reference polarity shift at the confusion point. Therefore, it is not advisable to fire the jets for orbital velocity change. However, if conservation of jet fuel or optimization of orbital change (with respect to time) dictates that the jets must be fired within a confusion area, the same effective result can be accomplished. Theoretically, this is possible by applying two jet thrust vectors which have an equivalent thrust resultant at the desired point within a confusion area.

Thus, an effective orbital change at a confusion point can be produced by properly firing jets just prior to and immediately after the satellite passes a confusion area. It may then be seen that orbital velocity changes can be accomplished at any point in the satellite orbit.

As mentioned previously, the satellite must rotate 180 degrees in yaw at each confusion point ($\Omega = 90^\circ$ or $\Omega = 270^\circ$) or once every 12 hours. This can be a controlled maneuver energized by a limit switch when the solar banks reach their maximum angular travel. With the assumption that the yaw loop does not become fully effective until 5 degrees beyond the confusion point, the vehicle's yaw angular velocity must be 180 degrees in 20 min. or .15 deg/sec. If a jet pair is fired at each confusion point to impart an angular impulse resulting in an angular velocity of .15 deg/sec., the yaw sensor will be properly aligned to its reference when the yaw loop becomes fully effective.

For steady-state operation the solar banks must rotate 180 degrees in 12 hours or its angular velocity must be .25 deg/min. Therefore, the solar bank drive loop can be relatively slow compared to the vehicle-attitude-control system. As mentioned previously, this is an advantage from the standpoint of minimizing vehicle disturbance because of solar-bank rotation. To always insure a relatively slow solar-bank drive loop, velocity limiting can be used. By using a proper amount of gear reduction between the drive motor and the solar-bank axle, a limited value of $\dot{\lambda}_{max}$ will result when the motor reaches maximum speed. This is illustrated by Figure 17 with $\dot{\lambda}_{max}$ arbitrarily equal to 1 deg/min. A limit switch is also shown to limit the maximum angular travel of the solar banks to $-90^\circ < \lambda < 90^\circ$. Also included is a tachometer feedback loop in the event that the motor back emf does not provide the desired loop damping.

Figure 18 gives an overall attitude-control-system block diagram less the complete jet back-up portions for the pitch, roll and yaw channels. All the previously mentioned rejection, compensating, and limiting networks are included. As an optional feature, a switch controlled by λ is shown as an input to the yaw gain compensation amplifier. Thus, the yaw gain may be switched to zero in the regions of yaw confusion although, theoretically, this is not necessary since the gain must fall to zero, as illustrated by Figure 14.

As developed in the previous progress report, it was shown that the angular momentum stored in the yaw and roll flywheels of the control system must be continuously exchanged at a frequency of one cycle per day. This is because of the controlled rotation of the satellite about its pitch axis as it orbits the earth every 24 hours. Since the satellite under consideration in this report has this same controlled rotation, its yaw and roll flywheel speeds must also vary sinusoidally with a 90° phase relationship. However, at the two confusion points, when the vehicle rotates 180° about the yaw axis, there

must also be a polarity shift in both the pitch and roll flywheel speeds because of the yaw rotation. Figure 19 illustrates a typical momentum exchange for the yaw, pitch and roll flywheels over a 24 hour interval. This illustration assumed no external disturbances and was plotted for initial flywheel speeds of 2,000 RPM, 1250 RPM and 0 RPM for yaw, pitch and roll, respectively. The transients in the flywheel speeds during the periods of confusion (denoted by the shaded areas) are not shown.

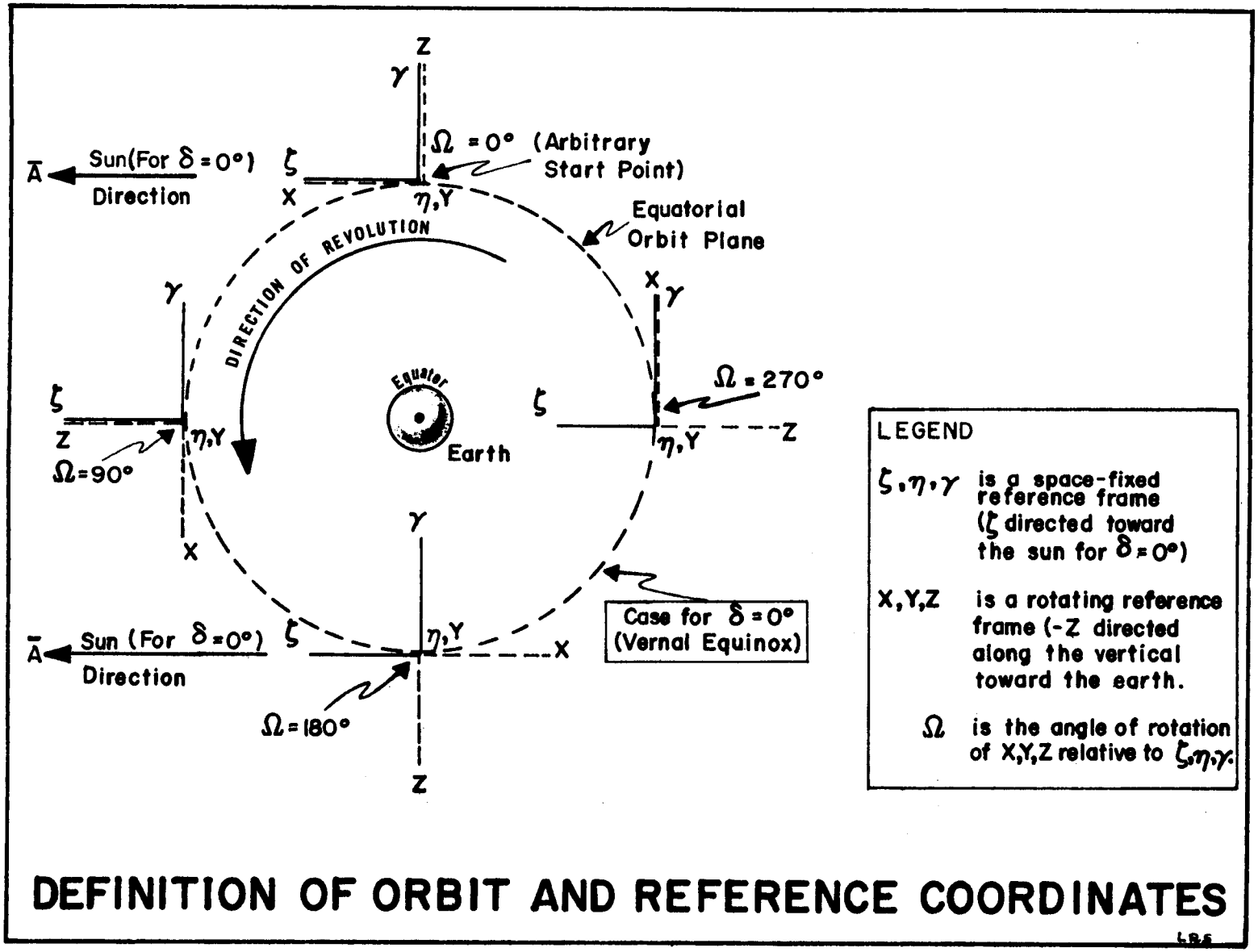

DEFINITION OF ORBIT AND REFERENCE COORDINATES

FIG. 1

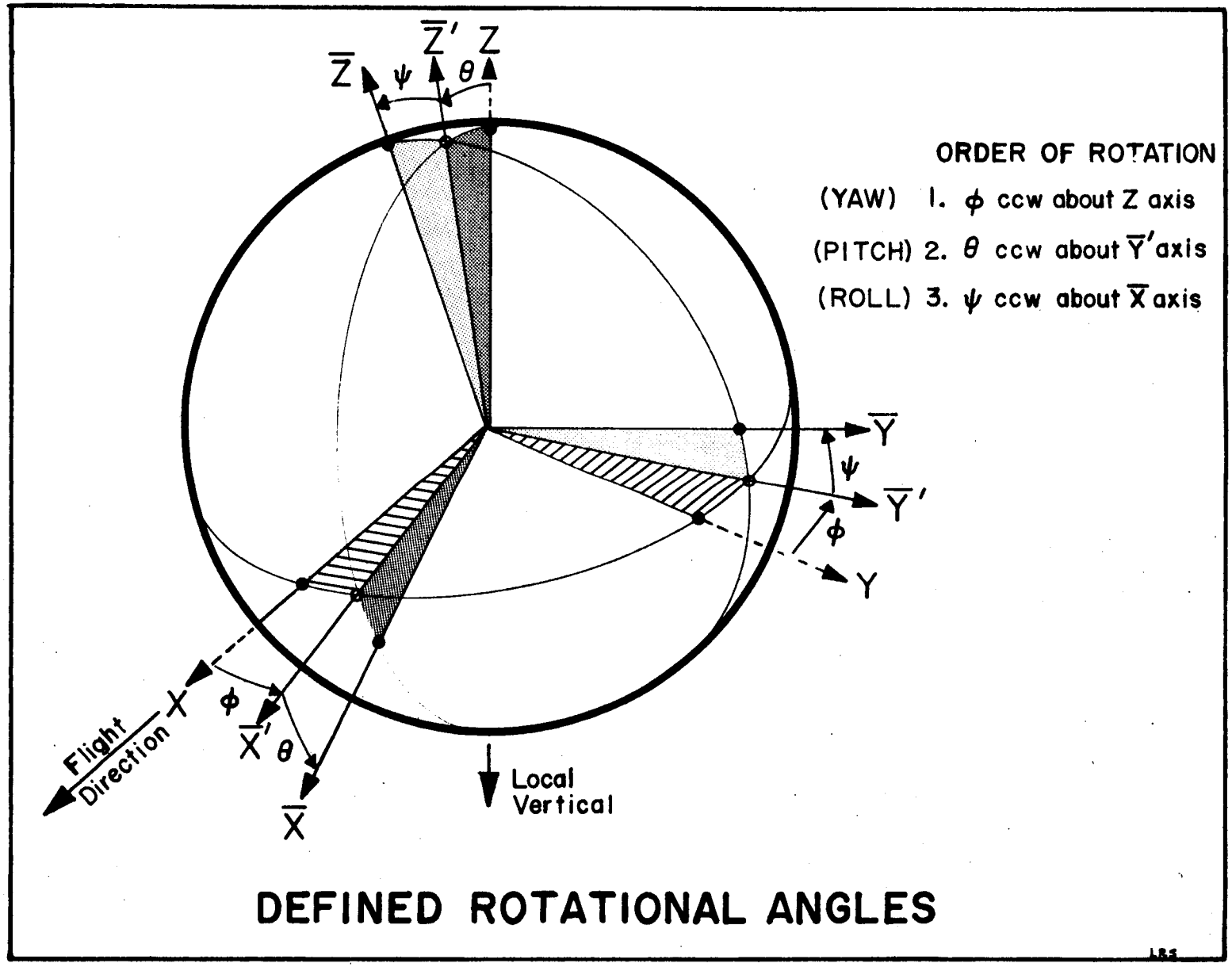

DEFINED ROTATIONAL ANGLES

FIG. 2

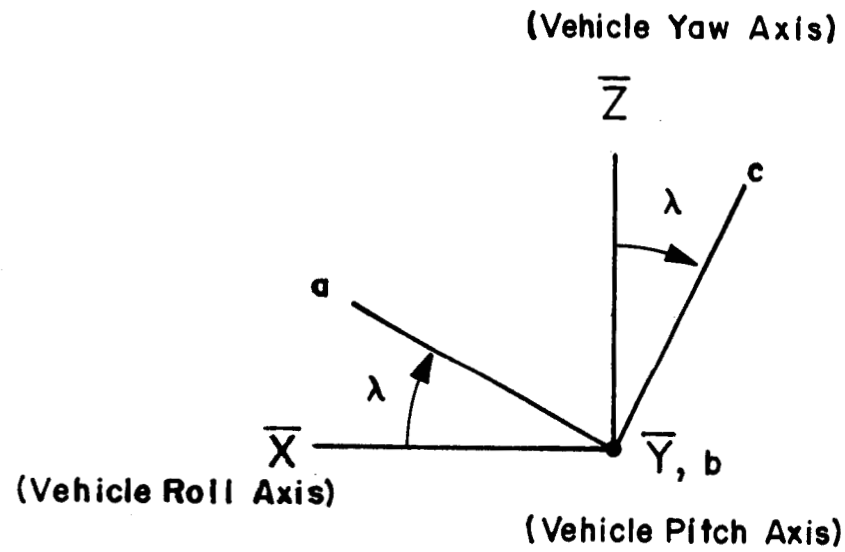

DEFINITION OF SERVO-DRIVE ANGLE λ ABOUT VEHICLE PITCH AXIS

FIG. 3

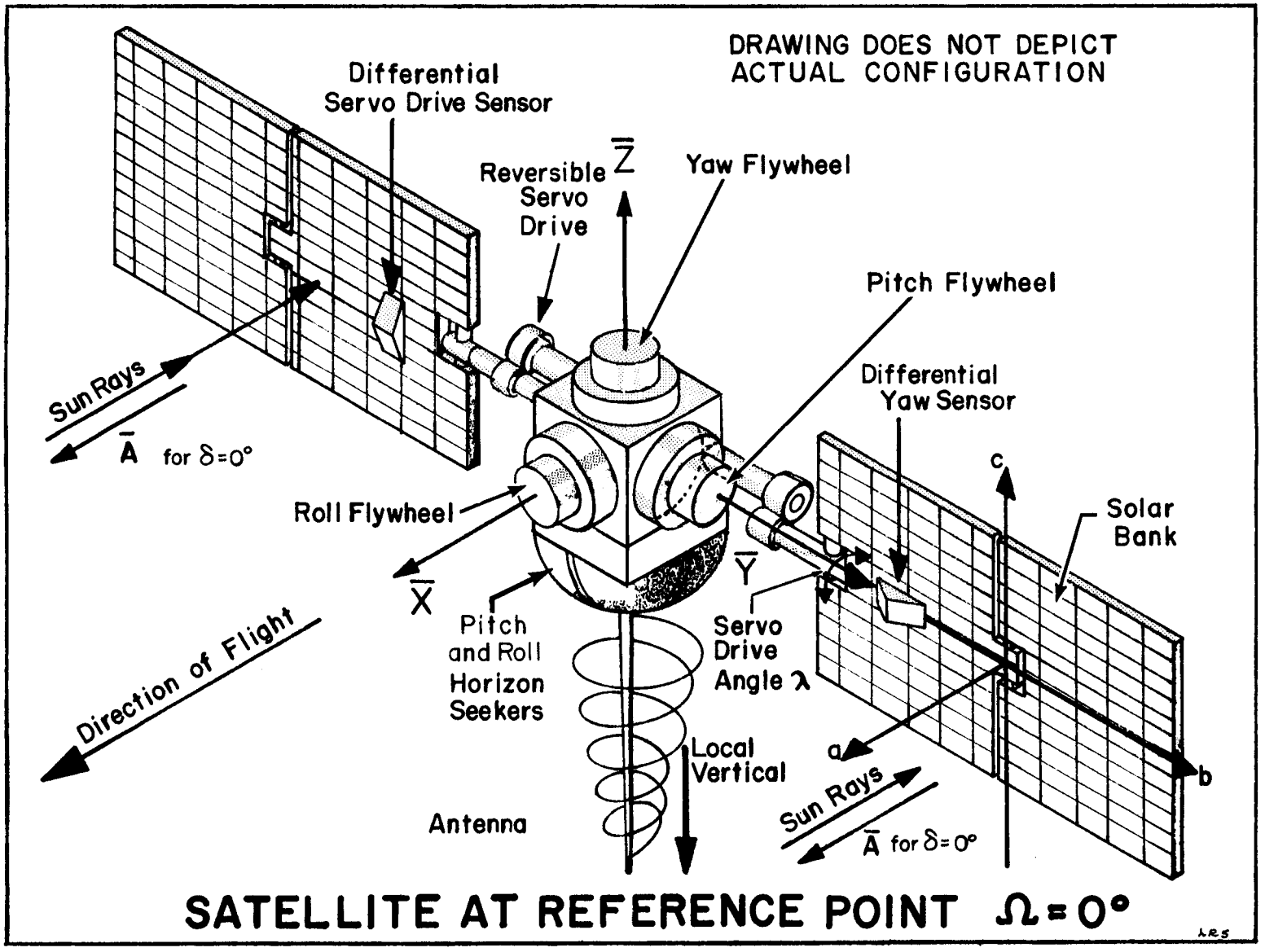
DRAWING DOES NOT DEPICT
ACTUAL CONFIGURATION
Differential
Servo Drive Sensor
Reversible
Servo
Drive
Z
Yaw Flywheel
Pitch Flywheel
Differential
Yaw Sensor
Sun Rays
A for δ=0°
Roll Flywheel
c
Solar
Bank
Y
X
Pitch
and Roll
Horizon
Seekers
Servo
Drive
Angle λ
Direction of Flight
Local
Vertical
a
b
Antenna
Sun Rays
A for δ=0°
SATELLITE AT REFERENCE POINT Ω=0°

FIG. 4

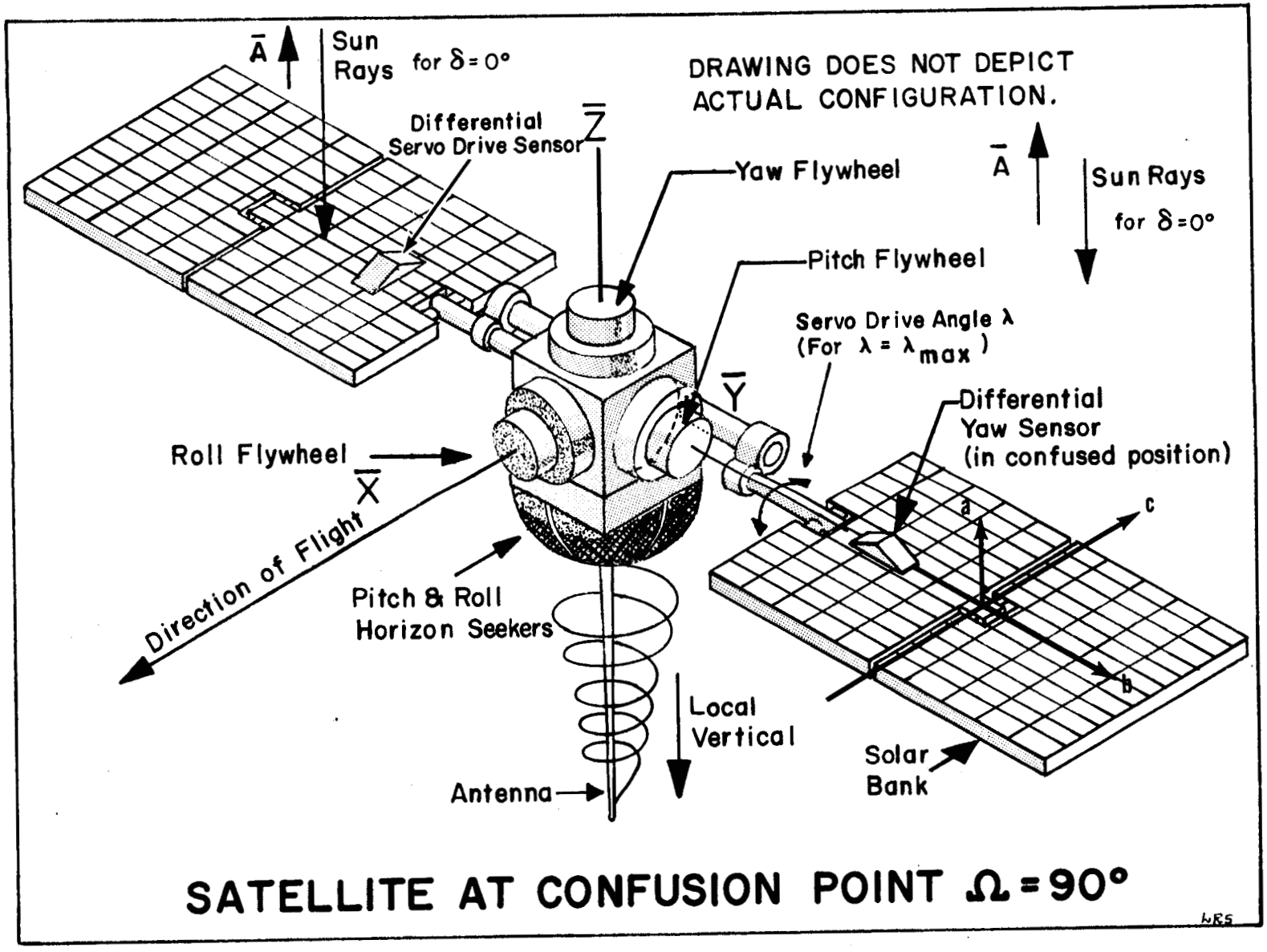
$\bar{A}$
Sun Rays for $\delta = 0°$
DRAWING DOES NOT DEPICT ACTUAL CONFIGURATION.
Differential Servo Drive Sensor
$\bar{Z}$
Yaw Flywheel
$\bar{A}$
Sun Rays for $\delta = 0°$
Pitch Flywheel
Servo Drive Angle λ (For $\lambda = \lambda_{max}$)
$\bar{Y}$
Differential Yaw Sensor (in confused position)
Roll Flywheel
$\bar{X}$
Direction of Flight
a
c
b
Pitch & Roll Horizon Seekers
Local Vertical
Antenna
Solar Bank
SATELLITE AT CONFUSION POINT $\Omega = 90°$
WRS

FIG. 5

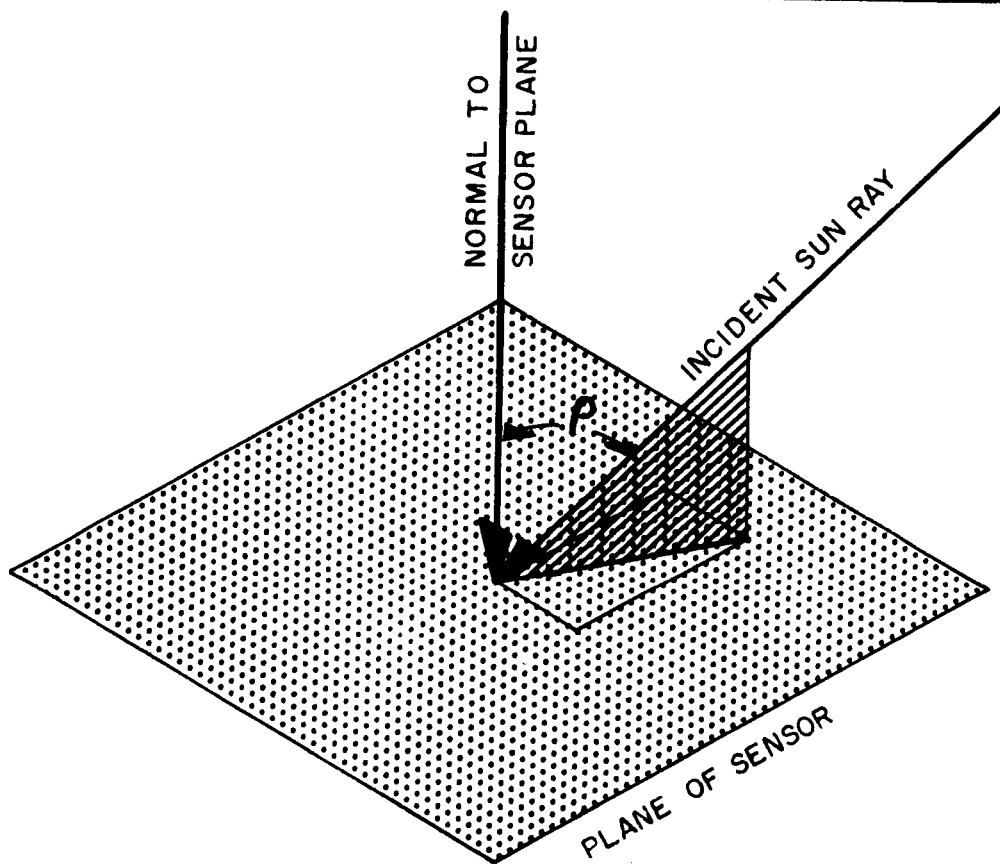

$$E = K \cos \rho$$

ILLUSTRATION OF SENSOR ELEMENT

LRS

FIG. 6

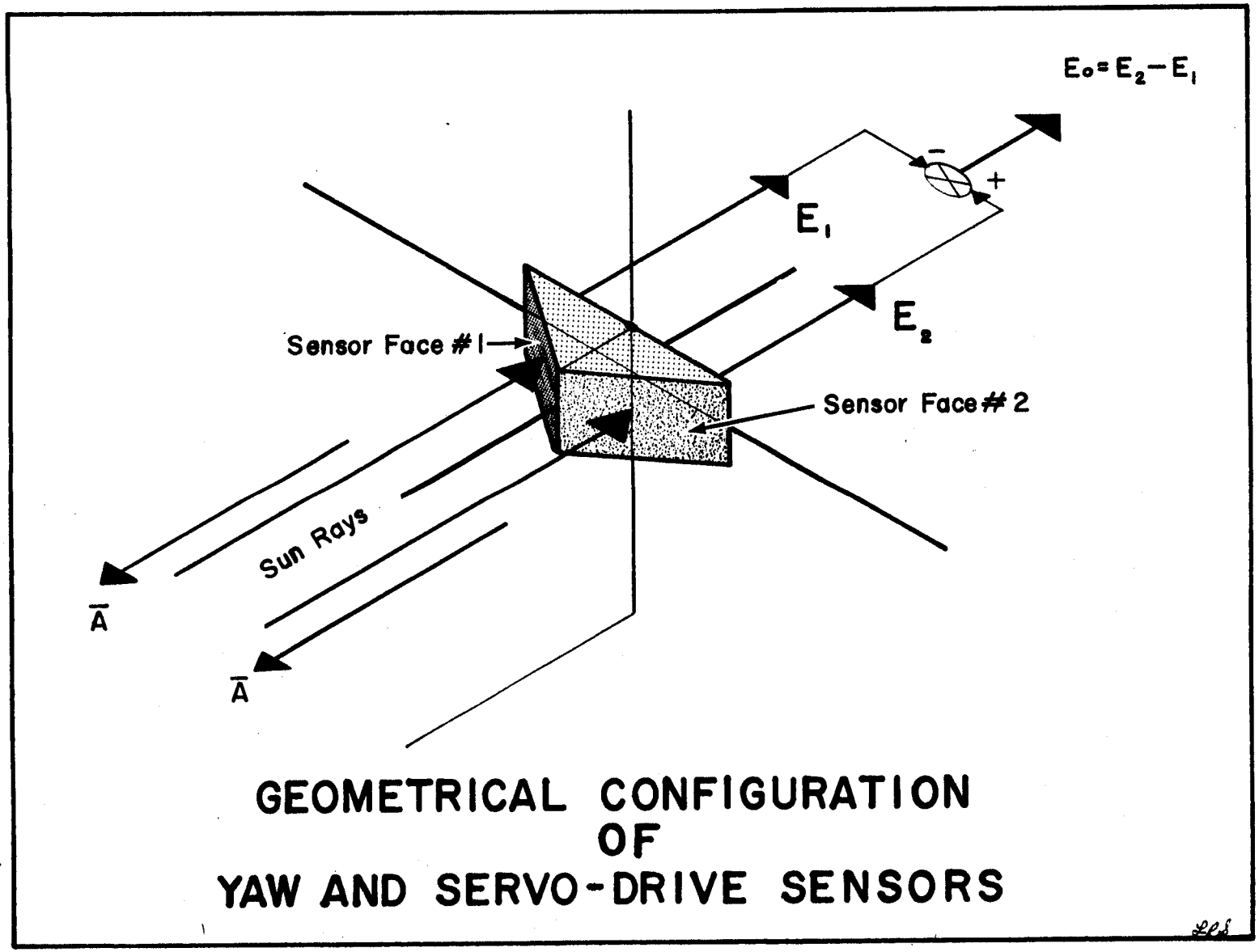

GEOMETRICAL CONFIGURATION
OF
YAW AND SERVO-DRIVE SENSORS

FIG. 7

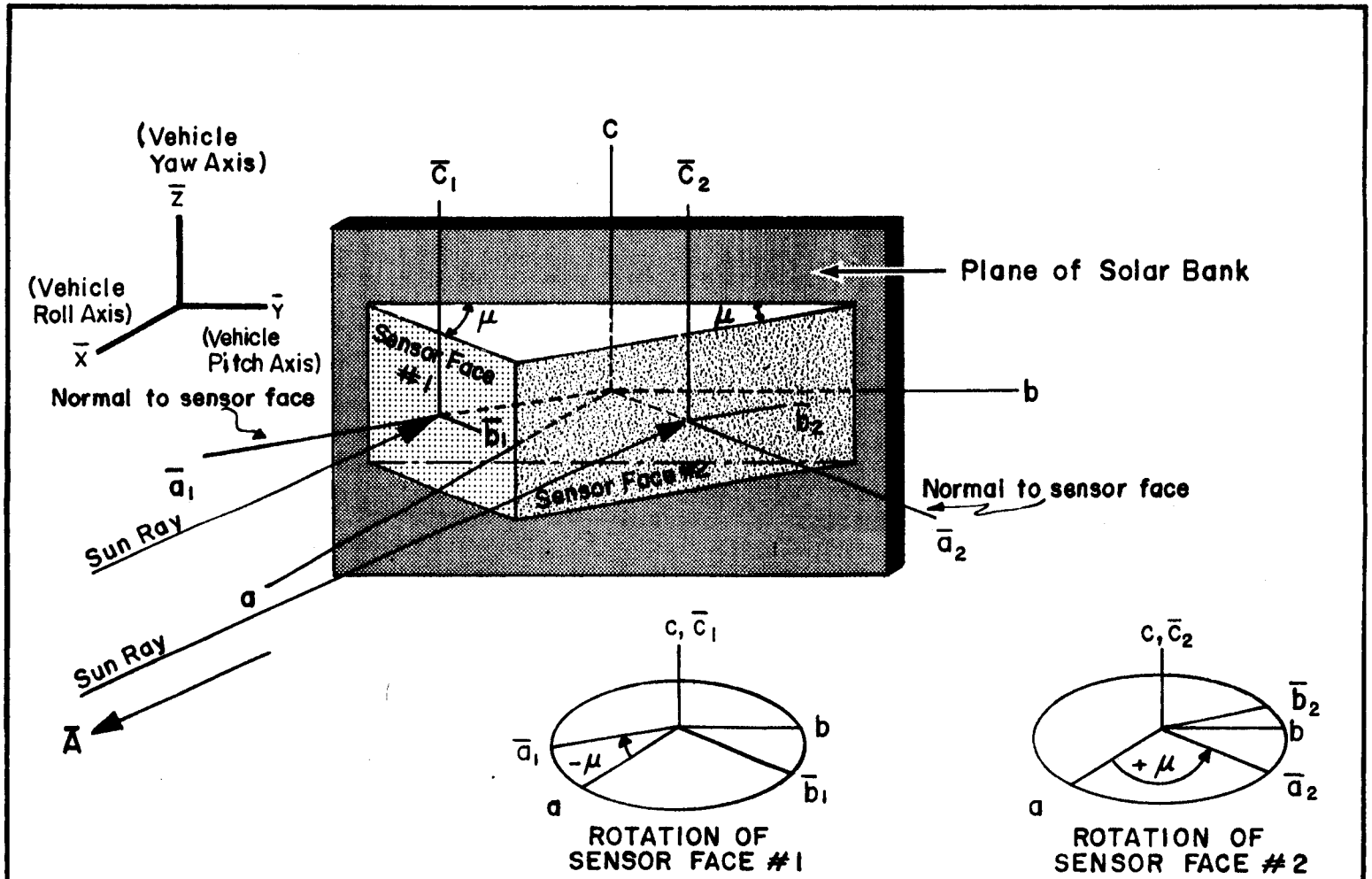

ILLUSTRATION OF YAW SENSOR

FIG. 8

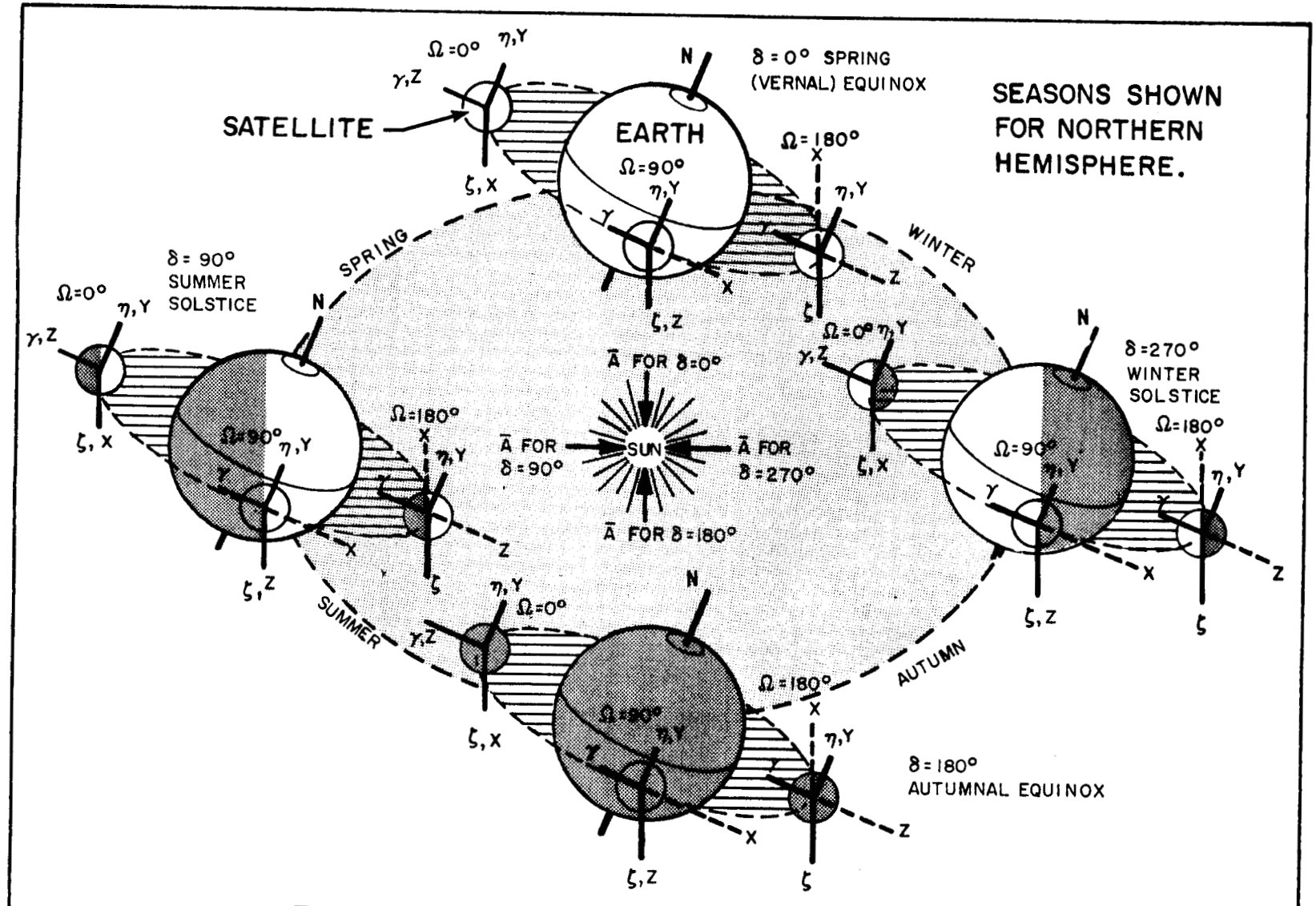

PICTORIAL REPRESENTATION OF REFERENCE COORDINATE SYSTEMS

FIG. 9

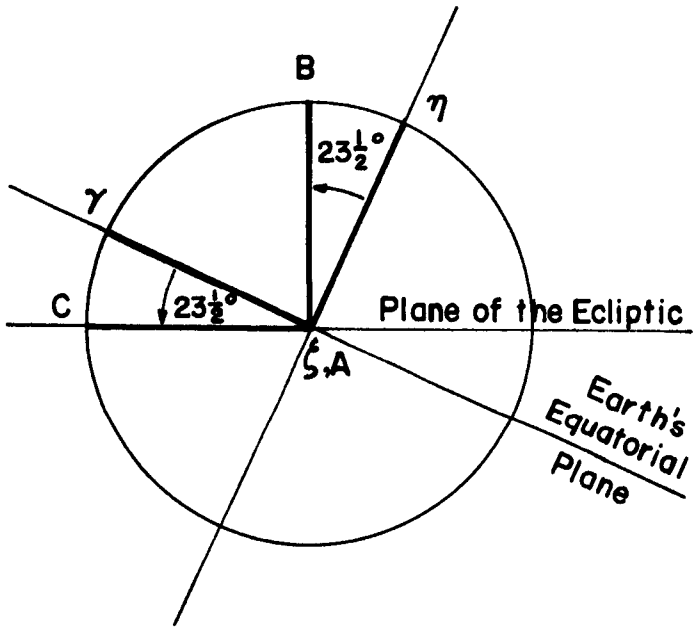

FIG. 10a
EQUATORIAL PLANE INCLINATION WITH RESPECT TO THE ECLIPTIC PLANE.

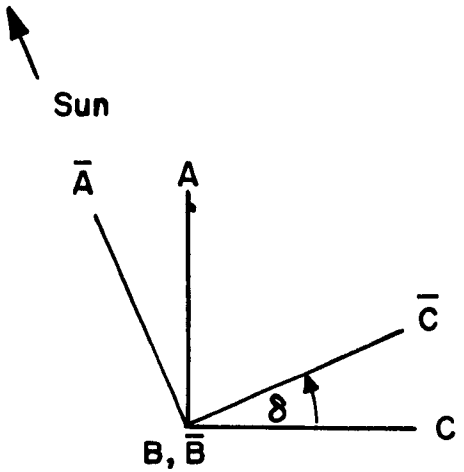

FIG. 10b
DEFINITION OF THE EARTH'S ORBITAL ROTATION ANGLE δ.

COORDINATE SYSTEMS TO DESCRIBE THE EARTH'S ROTATION ABOUT THE SUN

HKS

FIG. 10

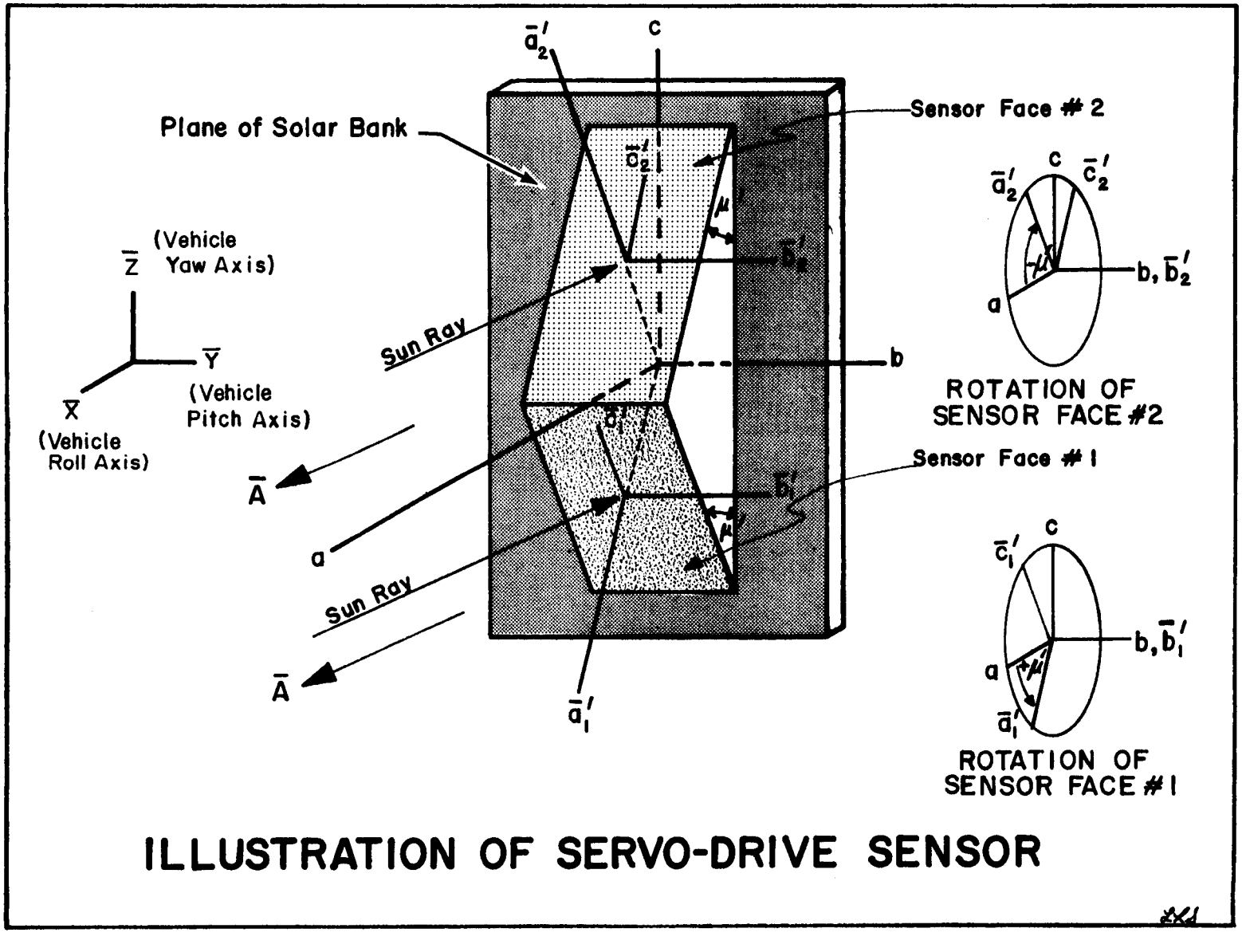
Plane of Solar Bank
Sensor Face # 2
Sensor Face # 1
(Vehicle Yaw Axis)
(Vehicle Pitch Axis)
(Vehicle Roll Axis)
Sun Ray
Sun Ray
ROTATION OF SENSOR FACE #2
ROTATION OF SENSOR FACE #1
ILLUSTRATION OF SERVO-DRIVE SENSOR

FIG. 11

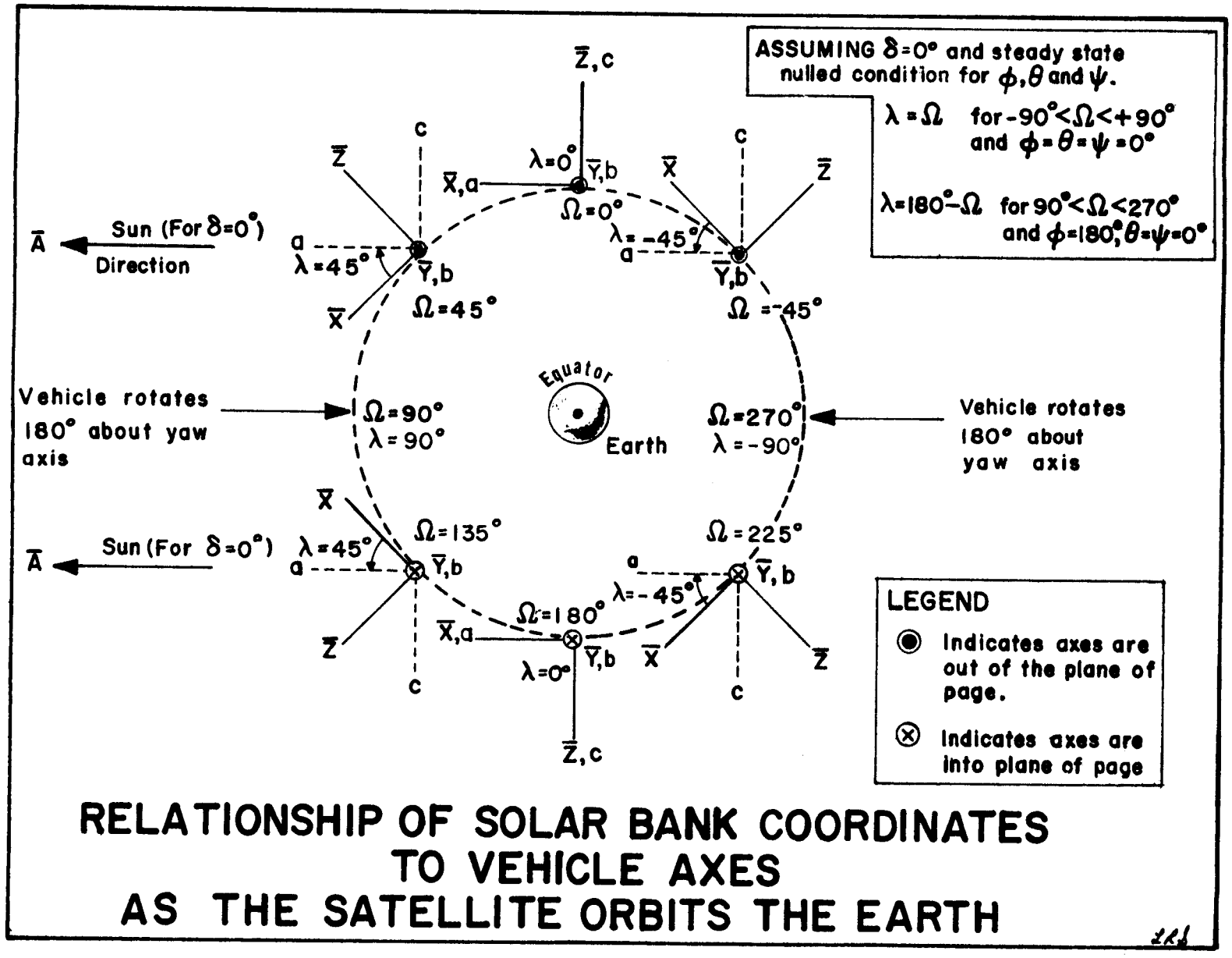

RELATIONSHIP OF SOLAR BANK COORDINATES TO VEHICLE AXES AS THE SATELLITE ORBITS THE EARTH

FIG. 12

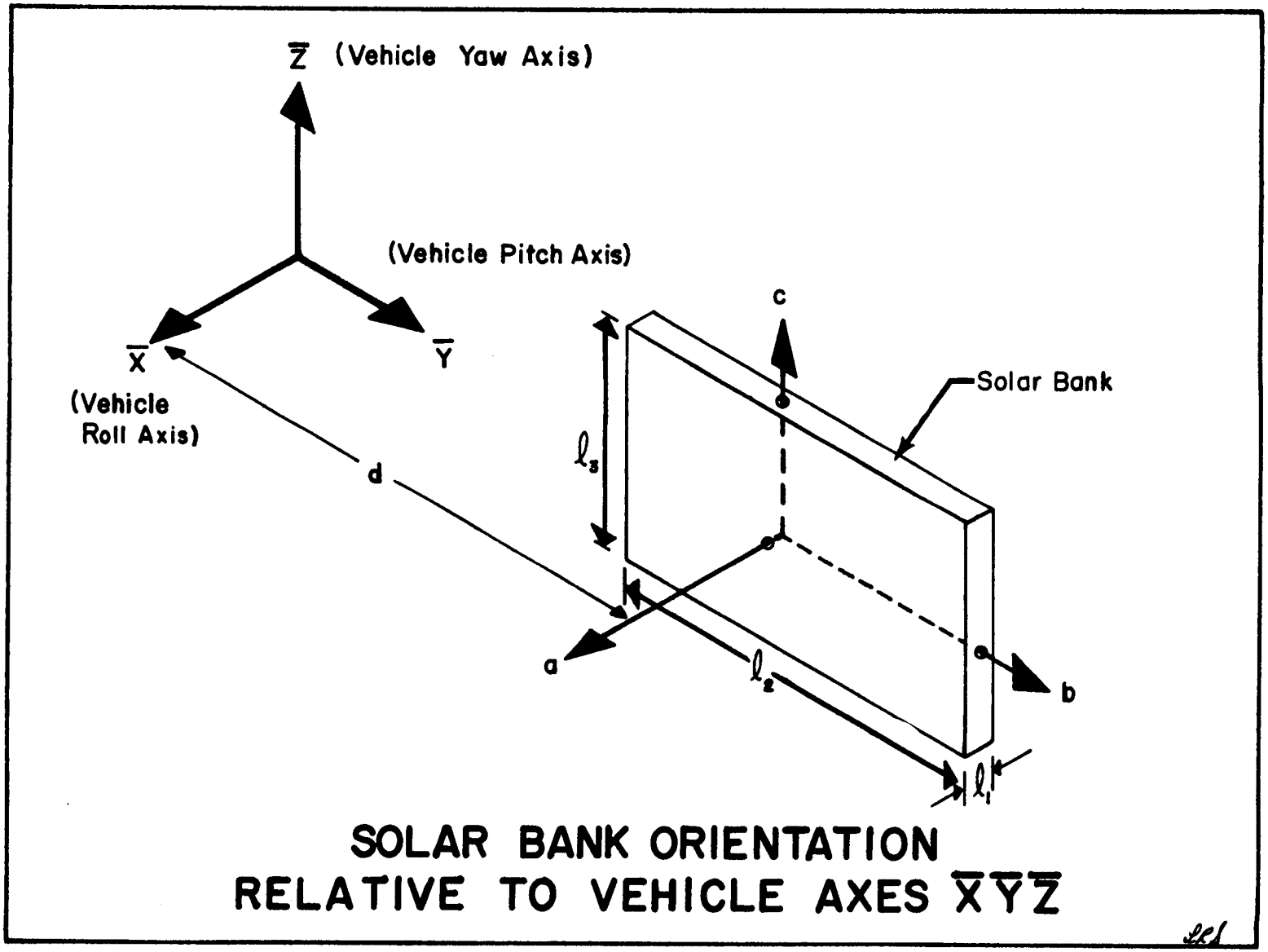
$\bar{Z}$ (Vehicle Yaw Axis)
(Vehicle Pitch Axis)
$\bar{X}$
$\bar{Y}$
(Vehicle Roll Axis)
d
c
Solar Bank
l_3
a
l_2
b
l_1
SOLAR BANK ORIENTATION
RELATIVE TO VEHICLE AXES $\bar{X}\bar{Y}\bar{Z}$

FIG. 13

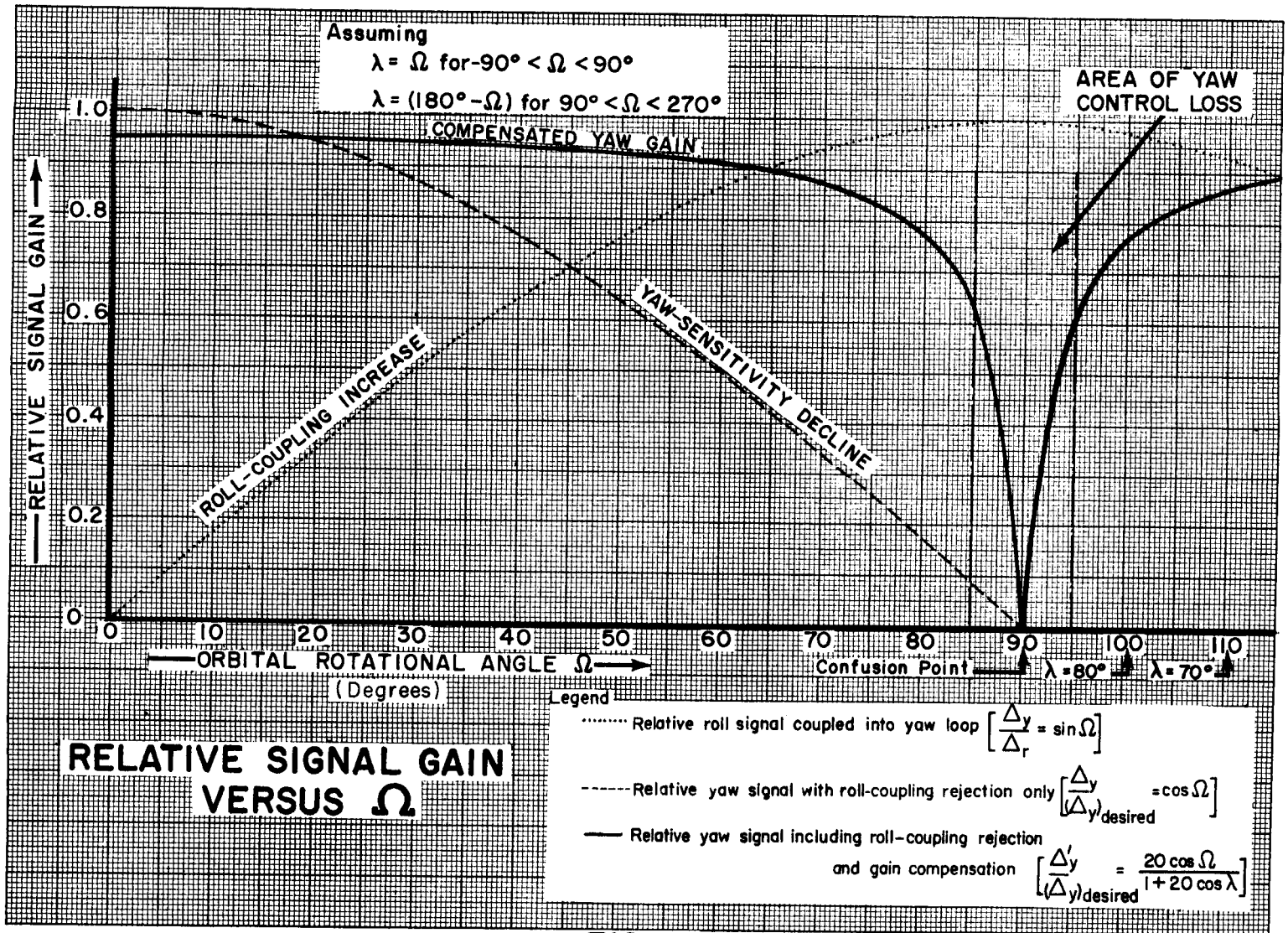
Assuming
λ = Ω for -90° < Ω < 90°
λ = (180° - Ω) for 90° < Ω < 270°
AREA OF YAW CONTROL LOSS
COMPENSATED YAW GAIN
ROLL-COUPLING INCREASE
YAW-SENSITIVITY DECLINE
RELATIVE SIGNAL GAIN
1.0
0.8
0.6
0.4
0.2
0
0
10
20
30
40
50
60
70
80
90
100
110
ORBITAL ROTATIONAL ANGLE Ω
(Degrees)
Confusion Point
λ = 80°
λ = 70°
Legend
Relative roll signal coupled into yaw loop [Δy/Δr = sin Ω]
Relative yaw signal with roll-coupling rejection only [Δy/(Δy)desired = cos Ω]
Relative yaw signal including roll-coupling rejection and gain compensation [Δ'y/(Δy)desired = 20 cos Ω / 1 + 20 cos λ]
RELATIVE SIGNAL GAIN VERSUS Ω

FIG. 14

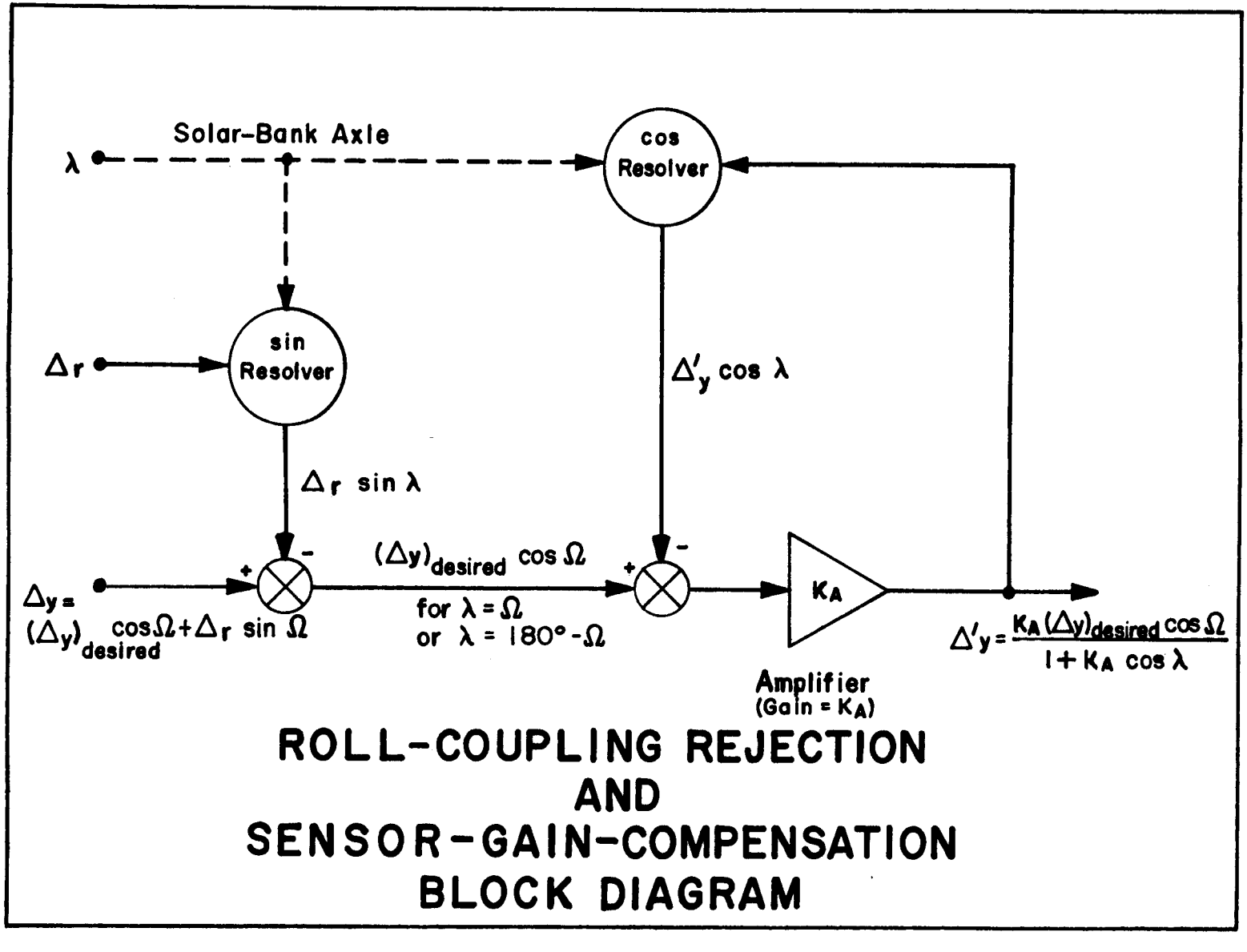

ROLL-COUPLING REJECTION AND SENSOR-GAIN-COMPENSATION BLOCK DIAGRAM

FIG. 15

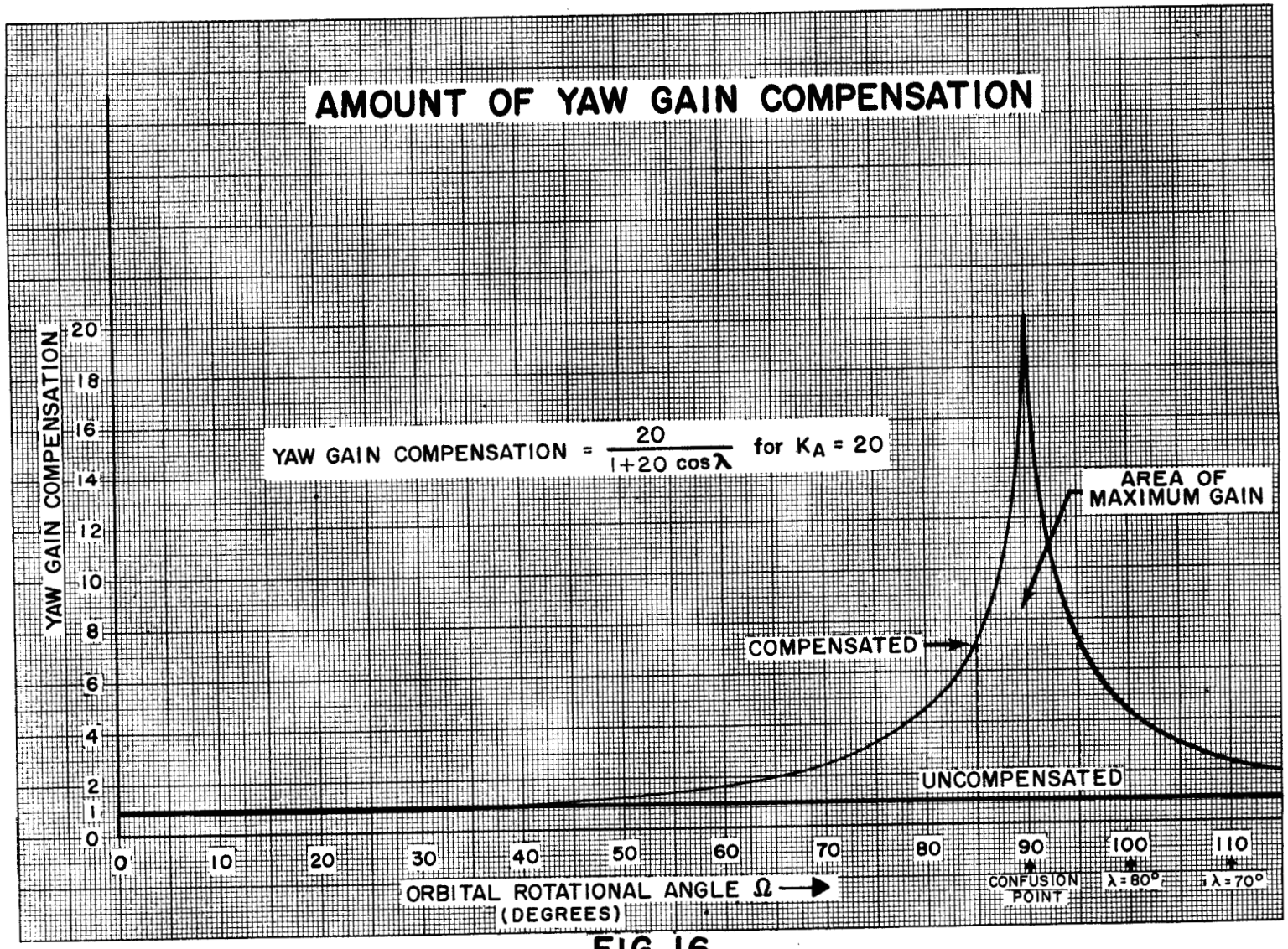
AMOUNT OF YAW GAIN COMPENSATION
YAW GAIN COMPENSATION
YAW GAIN COMPENSATION = 20 / 1+20 cosλ for K_A = 20
AREA OF MAXIMUM GAIN
COMPENSATED
UNCOMPENSATED
20
18
16
14
12
10
8
6
4
2
1
0
0
10
20
30
40
50
60
70
80
90
100
110
CONFUSION POINT
λ = 80°
λ = 70°
ORBITAL ROTATIONAL ANGLE Ω
(DEGREES)

FIG. 16

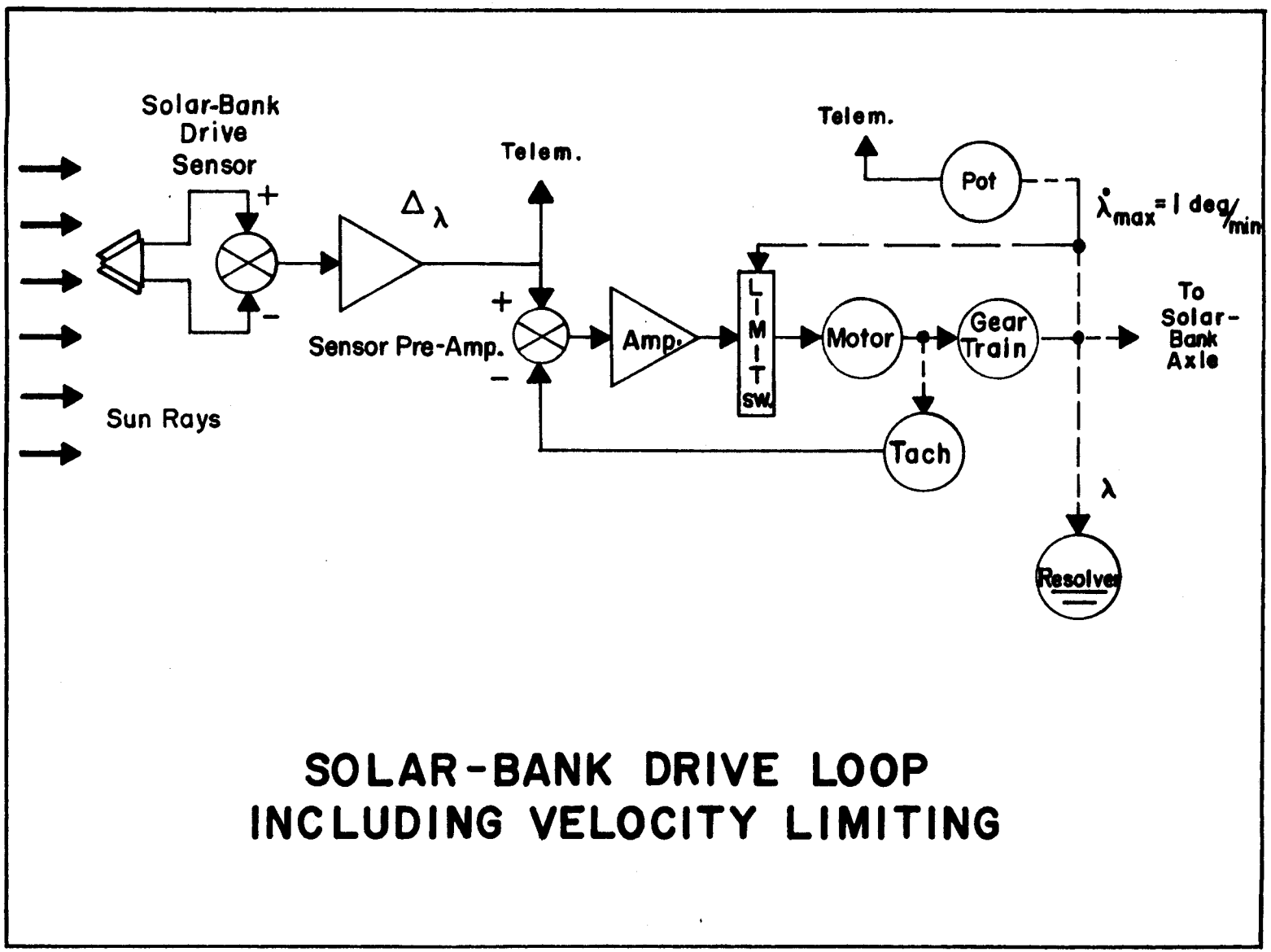

SOLAR-BANK DRIVE LOOP
INCLUDING VELOCITY LIMITING

FIG. 17

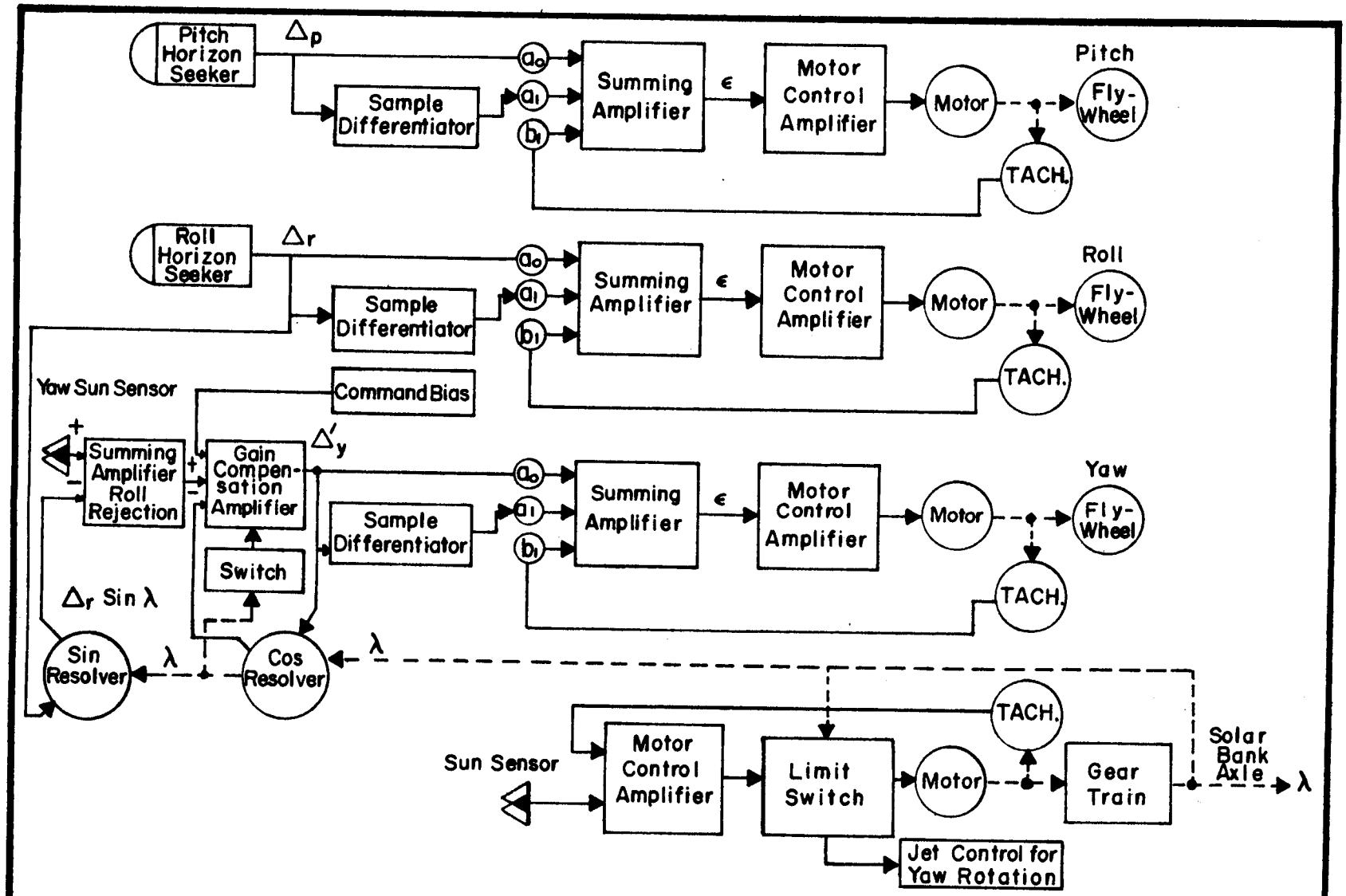

ATTITUDE-CONTROL-SYSTEM DIAGRAM

(LESS JET BACK-UP PORTIONS)

FIG. 18

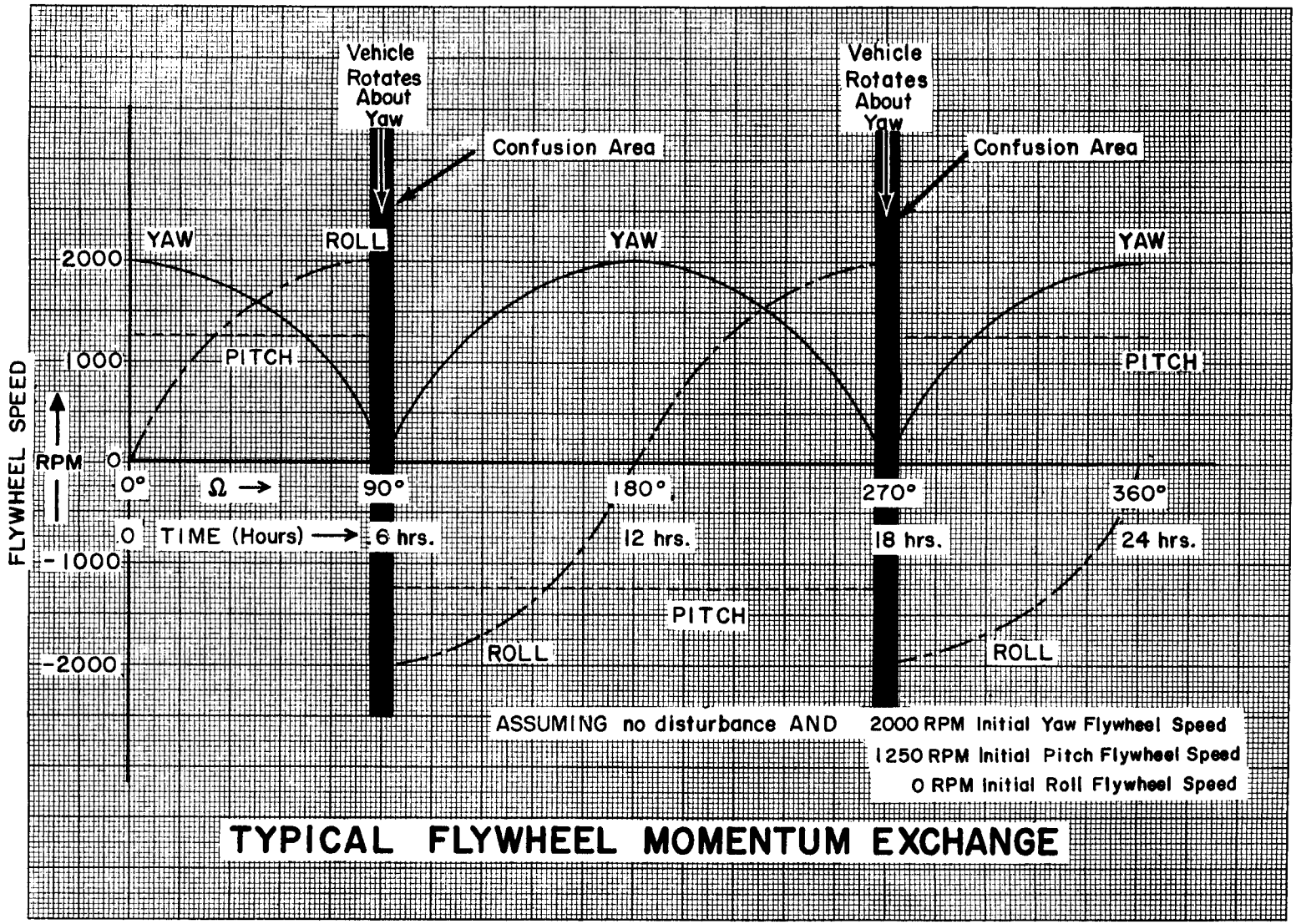
Vehicle Rotates About Yaw
Confusion Area
Vehicle Rotates About Yaw
Confusion Area
YAW
ROLL
YAW
YAW
2000
1000
PITCH
PITCH
FLYWHEEL SPEED
RPM
0
-1000
-2000
0°
Ω →
90°
180°
270°
360°
0
TIME (Hours) →
6 hrs.
12 hrs.
18 hrs.
24 hrs.
PITCH
ROLL
ROLL
ASSUMING no disturbance AND 2000 RPM Initial Yaw Flywheel Speed
1250 RPM Initial Pitch Flywheel Speed
0 RPM Initial Roll Flywheel Speed
TYPICAL FLYWHEEL MOMENTUM EXCHANGE

FIG. 19

DISTRIBUTION:

M-DIR Attention: Mr. Rees

M-FUT Attention: Mr. Koelle (2)

M-AERO-DIR Attention: Dr. Geissler

M-RP-DIR Attention: Dr. Stuhlinger (2)

M-G&C-DIR Attention: Dr. Haeussermann (2)
-N Attention: Mr. Moore
-NC Attention: Mr. Drawe
Attention: Mr. Kennel (3)
-NS Attention: Mr. Taylor
-A Attention: Mr. Digesu
-M Attention: Mr. Boehm

Mr. Webster
Mr. Schultz